CENTRO DE INVESTIGACIONES EN ÓPTICA, A.C.

Encapsulation of organic solar cells with polymeric resins, their PV performance and lifetime

TO OBTAIN THE DEGREE OF MASTER IN SCIENCE (OPTICS)

Presented by:

Luz-María García-Encina, B. Sc.

Under the supervision of:

José-Luis Maldonado-Rivera, Ph. D.

October 2016
León, Guanajuato,
México

Contents

Acknowledgments

This work was supported by different people and grants who I wish to thank. To CONACyT for providing my scholarship (565610) and particularly to the project CONACyT-SENER 153094 and CeMIE-Sol 207450/27 call 2013-02, Fondo Sectorial CONACYT-SENER SUSTENTABILIDAD ENERGETICA for the economic support. To Centro de Investigaciones en Óptica (CIO) where this master's studies took place. To José Luis Maldonado Rivera for his great guidance, support and patience. To all GPOM (Group of Optical Properties of Materials) members for their support and friendship, especially Denisse, Alvaro, Misael, Diecenia, Armando, Martin and Leonardo for the help they gave me in and out laboratory. To my parents, brothers, sisters in law and nephews, who believed in me and supported me all the time. To my thesis committee members Dr. Oracio Barbosa García and Dr. Enrique Pérez Gutiérrez, for reviewing this thesis and due to their fruitful comments that improved a lot this work.

Abstract

In this thesis UV-curable polymers (NOA 61, 65, 71, 76 and 138 from Norland Optics), were used for encapsulating organic solar cells (OPVs) to increase their lifetime and profitability. OPVs cells were encapsulated in either: a dry nitrogen glove box and under normal conditions (outside glove box). All devices were stored outside glove box with minimal lighting. Two ways of encapsulation were used: a) By covering OPVs with a glass cap (GCE) and b) by applying and sealing the adhesive directly on the cell top. Best results both outside and inside the glove box were reached with NOA 65 and NOA 71 resins through the GCE method and applying directly on the cell, respectively. After 46 days the efficiency of OPVs encapsulated under normal conditions decreased 50 % with the GCE method and 27% applying directly, while the test cell (without any encapsulated resin) decreased 64%. On the other hand, after 46 days the efficiency of OPVs encapsulated in a controlled atmosphere decreased 35% with the GCE method, 25% applying directly, and test cell decreased 51%, however theses OPVs devices stopped working after 57 days and the efficiency decreased 32% with the GCE method, 33% applying directly, and test cell decreased 62%. Based on the experimental results it was observed that the efficiency decrease less for OPVs encapsulated inside glove box (and tested outside); the used adhesives could provide an acceptable barrier against degradation caused mainly by oxygen and moisture.

Chapter 1

Introduction

Currently energy and environment have become two of the most critical subjects of wide concern, and these topics are also correlated to each other. An estimated 80% or more of today's world energy supplies are from the burning of fossil fuels such as coal, gas, or oil [1]. Due to today's increased demands for energy supplies coupled with increased concerns of environmental pollution, alternative renewable, environmentally friendly as well as sustainable energy sources become desirable. Several types of renewable energies, are: hydropower, biomass, wind energy, geothermal energy, marine energy, solar thermal energy and solar energy, especially solar cells.

Traditional solar cells are made of inorganic materials (silicon) however, the production cost is high, and rate at which new solar cell area can be produced is

limited by the basic high-temperature processing of silicon. Semiconducting polymers and organic materials provide an alternative route to solar cell technology [2].

For this reason solar cells based on organic materials (OPVs) have attracted strong attention in recent years, because the manufacturing process is not complicated, cheaper and their production methods are faster, compared to silicon cells. The materials used are cheap, easy to synthesize and properties can be tailored by molecular design. Due to the optical and electrical properties of OPVs, it is possible to make thin, semitransparent, lightweight and flexible solar cells. Among the current disadvantages of this technology can be mentioned: oxidation of organic materials through chemical reactions with water and oxygen, light irradiation deterioration, instability of active materials when devices not have any external encapsulation and lower maximum achievable efficiencies with respect those based on Si [3, 4] and, low absorption in the infrared (IR) spectral range. A commercial solar cell of crystalline Si has an efficiency about 25% [5], meanwhile in OPVs a maximum efficiency of 13% (under lab conditions) is reported [6].

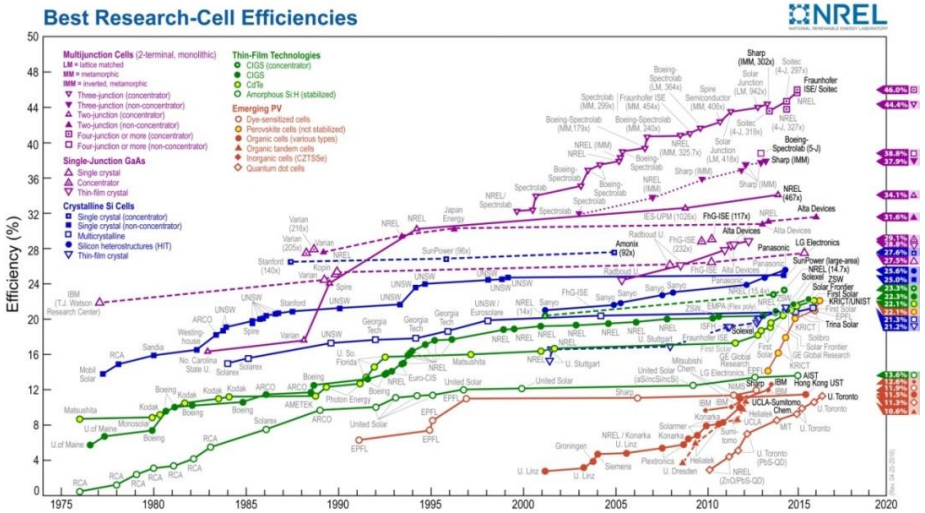

Figure 1.1 Best solar cell efficiencies reported to date [6].

The efficiency and the lifetime of OPVs are the main problems; however all these disadvantages can be overcome by changing the design of the OPVs. Inverted architectures [7] can be used to improve cell's stability, optical design and tandem structures [7] can be used to increase efficiency. This fact can be improved through the choice of materials, UV-filters and improved techniques and encapsulation materials. In this thesis we focus especially on the encapsulation of the devices. The type and quality of encapsulation play an important role in the stability and overall lifetime of the device by limiting the amount of oxygen and water molecules that permeate into the cell. In this thesis the NORLAN adhesives [8] are used to protect organic devices. These adhesives are cured when exposed to ultraviolet light, curing of these adhesives does not damage the lighting characteristics of devices, further, it is an economic method that does not need vacuum or heating process to encapsulate the devices, and provide a good transparency due to their optical characteristics (low index of refraction and colorless) useful for future applications.

1.1. History of solar cells

In Mexico, 67.3% of the CO_2 emitted comes from electricity generation, positioning it as the Latin American country that emits more greenhouse gases. Renewable energies, particularly solar energy, have a big advantage in Mexican territory because, by its geographical location, receives an average radiation of 5 kWh/m^2 [9]. For these reasons, Mexico is attractive for the development,

manufacture and use of solar energy systems to replace the current ones used for electricity generation.

Solar photovoltaic energy conversion is one-step conversion process, which generates electrical energy from light energy. The photovoltaic effect was first reported by Edmud Bequerel in 1839 when he observed that the action of light on a silver coated platinum electrode immersed in an electrolyte produced an electric current. Forty years later the first solid state photovoltaic devices were constructed by workers investigating the recently discovered photoconductivity of selenium. In 1876 William Adams and Richard Day found that a photocurrent could be produced in a sample of selenium when contacted by two heated platinum contacts. In 1894, Charles Fritts prepared what was probably the first selenium solar cell, obtaining an efficiency of 1 % selenium [10]. Phillip Lenard discovered the role of the frequency of light regarding the energy of the emitted electrons in 1904 [11]. In the late 1950 and early 1960, the laboratories Bell Telephone and Hoffman Electronics increased the efficiency of inorganic silicon solar cells from 4 % to 14 %. In the 70's (semi)conducting polymers were discovered [10, 11]. Organic semiconductors are carbon-based materials possessing semiconductor characteristics. Ching Tang in 1986 publishes his work *Two layer organic photovoltaic cell* [12] and reported an efficiency of 1%. Tang described a two-layer device that employed copper phthalocyanine (CuPc) as the donor and a perylene tetracarboxylic derivative (PV) as the acceptor [6, 13]. In 1990 the “bulk-heterojunction” (BHJ) approach was developed [7], which consist on the blend of both donor and acceptor materials into a single active film, thus increasing efficiencies. Figure 1.2 shows the difference of bilayer and bulk heterojunction active layers. In 2000 year Allan J. Heeger, Alan G. MacDiarmid, and Hideki Shirakawa received the Nobel Prize in chemistry for the discovery and development of these conductive polymers.

As an alternative to conventional organic cells, based on semi-conductor materials they are hybrid cells. Devices employing dye-sensitized, nanocrystalline inorganic materials based on a photoelectrochemical process that was first developed by Grätzel in 1991. In 2012 it was reported for the first time a Hybrid organic-inorganic perovskite solar cells with a PCE 21% was shown in 2016 [4, 14].

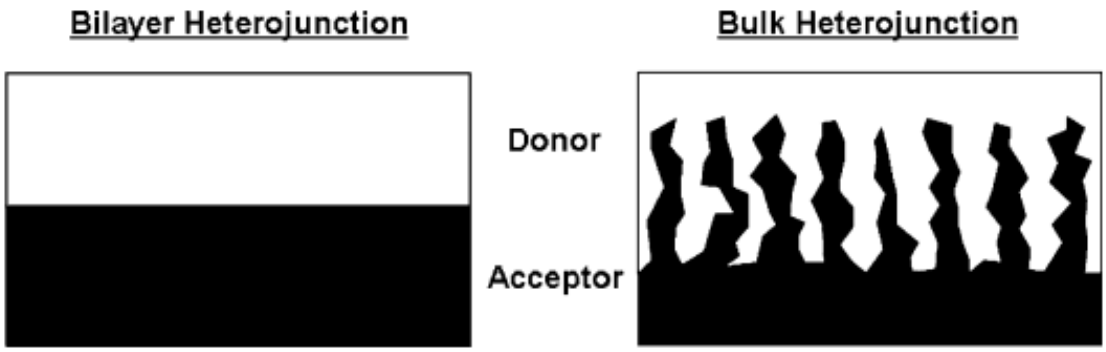

Figure 1.2 Difference of bilayer and bulk heterojunction active layers [13].

In the following years, several organic photovoltaic devices were reported [14, 15]. Recently, OPVs efficiency reached 13% [6]. The reason for this boom can be found in the expected high potential of organic semiconductors, which are either small molecules or polymers. Several techniques and a variety of materials have been used to accomplish the architecture of the devices. The most common technique is simply to disperse fullerene, or one of its derivatives, in a conjugated polymer and then spin-coated the solution onto the device.

Nerveless, OPVs deteriorate because the organic materials are by nature more susceptible to chemical degradation by oxygen and water molecules than

inorganic materials, which lead to a reduced reliability and lifetime of devices under normal environmental conditions. For this reason it is important the study of more stable photoactive layers through the introduction of additives, optimization of polymer synthesis routes to minimize incidence and concentration of impurities, and post-synthesis purification treatments and very remarkably: the development of superior quality encapsulation technologies to limit oxygen and moisture permeation from the environment into device layers [12]. Organic encapsulation materials offer significant advantages including flexibility in the synthesis of the organic, which allows parameters such as the molecular weight, energy levels, bandgap and solubility to be altered [11, 13].

1.2. Organic solar cells

A solar cell is a device by which electrical energy can be obtained directly, and by its nature, is modeled as a current generator. Light is made up of packets of energy, called photons, whose energy depends only upon the frequency, or color, of the light. The energy of photons in the visible region of the radiation is sufficient to excite electrons; photons are given up to excite electrons to higher energy states within the material. The process of converting light into electric current in an organic photovoltaic cell is accomplished by four consecutive steps: *Absorption* of a photon leading to the formation of an excited state, the electron-hole pair (exciton), *Exciton diffusion* to a region, where the *charge separation* occurs and finally the charge transport to the anode (holes) and cathode (electrons), to supply a direct current for the consumer load.

An OPV is generally composed of five layers (Figure 1.3) staked on the surface of a supporting substrate, which is normally a piece of glass or transparent plastic, these five layers include a transparent conductive electrode (anode), a hole transport layer (HTL), one photoactive layer (PAL) composed of an electron donor and an electron acceptor, an electron-transport layer (ETL), and a top metal electrode (cathode).

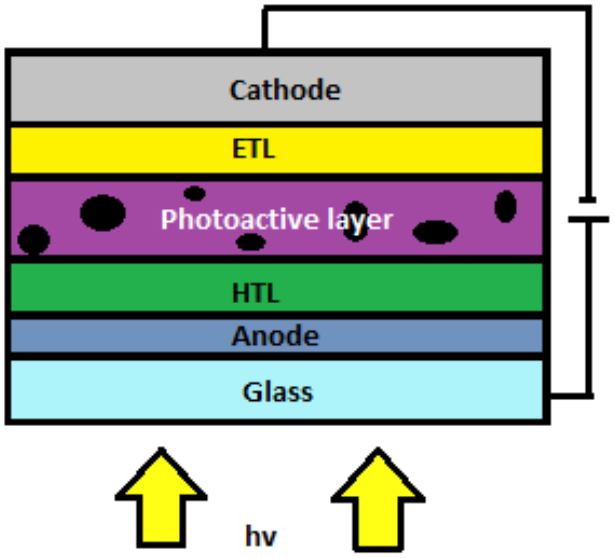

Figure 1.3 Cross section of a OPV with bulk heterojunction structure.

When a photon strikes an organic material and the frequency of the photon is appropriate, photon energy is absorbed by one of the electrons of the material reaching an excited state forming a pair of charges (electron and hole) inside the material. The bound state of the electron and hole is called exciton. Excitons are not stable states and only exist for short periods of time before recombined and

release the absorbed energy in the form of another photon. OPVs absorb most of the incident radiation to form excitons to separate after these excitons. Figures 1.4 represent the overall functioning for load generation, it is when photo-excited electrons remain loosely bounded to the positive charges (holes) even after being excited, needing another stimulus to completely separate the charges. This stimulus is provided by the electric field appearing at the interface of the two electron-donor (conjugated polymers) and electron-acceptor (fullerenes) materials, which drives the movement of electrons and holes in opposite directions, breaking the bound and directing them towards different electrodes.

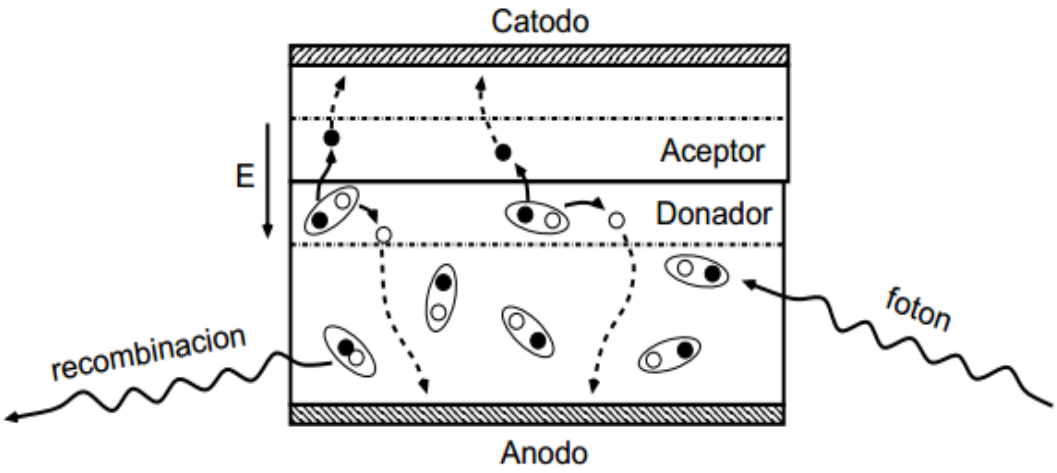

Figure 1.4 Cell process model of charge generation. Light stimulates an active medium generating excitons. A photon is absorbed by an electron donor material forming an exciton. If the bound state is formed of a donor-acceptor interface, the exciton has chance to dissociate into free charges (holes and electrons).

In amorphous organic materials like the ones used for solar cells, the absence of crystalline structure implies there is no conduction and valence bands like happens with their inorganic counterparts, nevertheless, energetic levels known as LUMO (lowest unoccupied molecular orbital) and HOMO (highest occupied molecular orbital) plays in organic materials a similar role to the conduction and valence bands in inorganic materials respectively [16, 17].

The HOMO and LUMO of organic semiconductors refer to energy bands that correspond to different hybridization states of the p-bonds, which will result in different energy levels of an organic semiconductor. When an electron is excited from the HOMO to the LUMO of an organic semiconductor, the molecule itself is excited into a higher energy state, as opposed to the actual excitation of a free electron from the valence band to the conduction band in inorganic semiconductors [16].

1.3. Solar cell characterization

The solar cell can take the place of a battery in a simple electric circuit. Devices are generally characterized by the *short-circuit current* density (J_{sc}), it is the current that flows through an illuminated solar cell when there is no external resistance. Represents the number of charge carriers that are generated and eventually collected at the electrodes at short circuit condition, the *open-circuit voltage* (V_{oc}) dependent on the energy difference of the acceptor LUMO and donor HOMO, the *fill factor* (FF) represents dependence of current output on the internal field of the device and is quantified by the series resistance and shunt resistance

and *maximum power point* (P_{max}), which is the point on the J-V curve where the maximum power is produced.

Figure 1.5 shows a schematic diagram of the current-voltage curve of a photodiode (solar cell) under illumination. The voltage developed when the terminals are isolated is called the *open circuit voltage* V_{oc}. The current drawn when the terminals are connected together is the short circuit current J_{sc}. The V_{oc} is the voltage where the JV curve crosses the horizontal axis (J = 0), J_{sc} is the current where the JV curve crosses the vertical axis (V = 0), V_{max} and J_{max} are respectively the voltage and current density of the point whose generated power is maximum among all the JV curve points ($P_{max} = V_{max}\ J_{max}$), the maximum power point is the point on the J_{max}-V_{max} curve where the area of the resulting rectangle is the largest.

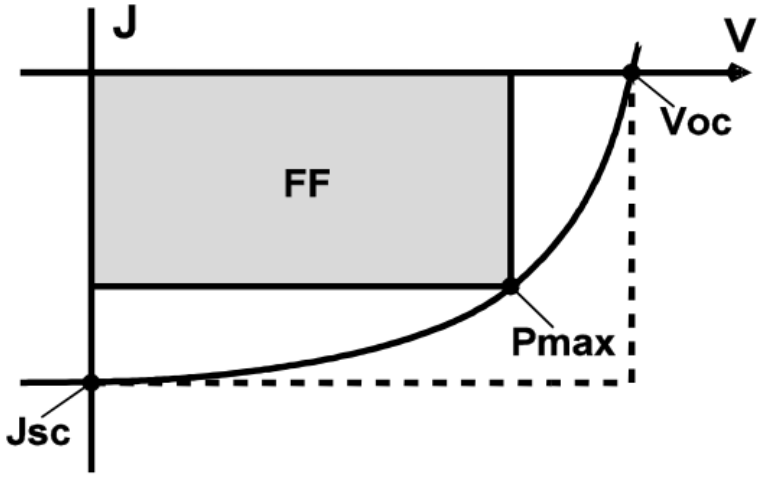

Figure 1.5 JV graph for a typical solar cell under illumination. Geometrically, the Fill Factor (FF) is defined as the ratio between the maximum power output point and the maximum attainable power output. The open circuit voltage (V_{oc}) and short-circuit current density (J_{SC}) are the characteristic intersections with the abscissa and the ordinate, respectively .

$$FF = \frac{V_{max} J_{max}}{V_{oc} J_{sc}} \quad (1)$$

as shown above, FF is the ratio between the maximum power output point and the maximum attainable power output. *Power conversion efficiency* (PCE) represents the efficiency of the solar cell and it is defined as:

$$PCE = \frac{FF\ V_{oc} J_{sc}}{P_{in}} \quad (2)$$

Where Pin stands for the luminous incident power on the cell, since there are several kinds of solar cells, a standard illumination that allows comparing among all those types is needed. This standard is called Air Mass 1.5 or AM1.5 and consists on the sun's illumination in a clear day when the ratio between the optical paths crossed by the sun's light in the atmosphere and the thickness of the atmosphere at the level of sea is equal to 1.5. This is achieved when the angle between sun and the zenith is approximately 48°. Experimentally this condition is impractical since it relies on having a clear day with fixed power intensity. A solar simulator is a device that replicates the Sun's emission spectrum under the AM1.5 condition using a fixed 100 mW/cm^2 luminous intensity.

1.4 Encapsulation of OPVs devices

Encapsulation methods play an effective role for improving the stability of OPV devices. These methods acts as a barrier layer by restricting the diffusion of oxygen and moisture through the organic material of the OPV devices, resulting in the protection of the organic/cathode interface and the active layer from deterioration. It also works to decrease the degradation of OPV devices.

The materials used for encapsulation have to meet the requirements of good processability, high optical transmission, high dielectric constant, low water absorptivity and permeability, high resistance to ultra-violet (UV) degradation and thermal oxidation, good adhesion, mechanical strength, and chemical inertness [18, 19]. Water vapor transmission rate (WVTR) and oxygen transmission rate (OTR) are the steady state rates at which water vapor and oxygen (respectively) gas can penetrate through a film that affects the encapsulation layer. A list of these requirements and specifications is given in Table 1.1 [19].

Table 1.1 Specifications and requirements for encapsulating materials.

Characteristics	Specification of requirement
WVTR	10^{-3}-10^{-6} g/m^2/day
OTR	10^{-3}-10^{-5} cm^3/m^2/day/atm
Total light transmission	>90% of incident light
Water absorption	<0.5 wt% (20°C,/100% RH)
Tensile modulus	<20.7MPa (>3000psi) at 25°C
UV absorption degradation	None (>350nm)

The oxygen transmission rate (OTR) is calculated by measuring the amount of oxygen during a certain period of time at a constant rate that it passes through the cathode. To determine the value of OTR it is necessary to use a colorimetric sensor [19-21]. Knowing the value of WVTR is possible to determine how good is the encapsulated performances, since it is possible to determine the degree of degradation that OPVs can have throught their lifetime and performance. The effective WVTR can be determined by monitoring the temporal rate of change of the cathode (calcium) electrical conductance through the use of the following equation [22-25].

$$\mathrm{WVTR}[\mathrm{g^{-1}m^{-2}day^{-1}}] = -\mathrm{n}\delta_{\mathrm{Ca}}\rho_{\mathrm{Ca}}\frac{\mathrm{d(G)}}{\mathrm{dt}}\frac{\mathrm{l}}{\mathrm{w}}\frac{\mathrm{M(H_2O)}}{\mathrm{M(Ca)}}\frac{\mathrm{Area\ (Ca)}}{\mathrm{Area(Window)}}$$

where, n is the molar equivalent of the degradation reaction with water, δ_{Ca} is cathode density, ρ_{ca} is cathode resistivity, G is the cathode conductance, $\mathrm{M(H_2O)}$ is the molar mass of water vapor and $\mathrm{M(Ca)}$ is the molar mass of cathode. The value of $\frac{\mathrm{d(G)}}{\mathrm{dt}}$ is calculated from the slope of a linear fit to the conductance versus time data.

For good OPVs protection, materials used as a barrier (encapsulant) should have a value larger than 10^{-6} g/m^2/day for WVTR (see Table 1.1), OLEDs unlike the materials must have a value of 10^{-6} g/m^2/day [17]. For instance, OPVs devices with the structure ITO/ZnO/P3HT:PCBM/PEDOT:PSS/Al were encapsulated using ZnO and UV resin with a large WVTR value of 5.0 x 10^{-1} g/m^2/day [25]. In Ref. [26] the WVTR value was as big as of 100g/m^2/day for an encapsulated OPV

(ITO/PEDOT:PSS/P3HT:PC71BM/Ca/Al) with an epoxy resin. On the other hand, in Ref. [21] OPVs cells under the configuration PET/DMD/Cs2CO3/P3HT:PCBM/MoO3/Al were encapsulated using polyvinyl butyral (PVB), ethylene vinyl acetate (EVA), and thermoplastic poly-urethane (TPU) with a WVTR value of 60 g/m^2/day, 40 g/m^2/day and 150 g/m^2/day, respectively, and with an OTR value in the range of 10^{-2}–10^2 cm^3/m^2/day. In this current work the WVTR and OTR values were not calculated due to different experimental details**.**

The most common type of an encapsulation method refers to thin film layers encapsulated on top of OPV devices using atomic layer deposition (ALD) [27]. ALD is particularly suitable for organic and flexible electronics. However, the ALD technique is expensive. Other methods are roll lamination systems encapsulating the OPV between two sheets uniting them with an adhesive [28], other method is based on heat sealing, a process which basically consists of supplying thermal energy on outside of package to soften/melt the sealants [21] and using a glass substrate that is to be sealed with thermosetting epoxy, it could not be effectively applied to flexible devices [29], among others [22, 30-40].

1.5 Degradation of OPVs devices

Low manufacturing costs of OPVs can replace negative aspects. Such profound discrepancy in device life expectancy between inorganic and organic PV cells stems from relatively high susceptibility of organic materials to water vapor and oxygen, which lead to reduced reliability and lifetime of organic devices under normal environmental conditions.

Depending on exposure, the degradation of OPVs can be divided into intrinsic and extrinsic. This can be due to air inside OPVs. Both types of degradation are mass-transport processes. The metal organic interfaces are the major interfaces where degradation occurs, even in OPVs that are stored in an inert atmosphere [40, 41].

Intrinsic degradation due to changes in the characteristics of the interfaces between layers of the stacking owing to internal modification of the materials used.

Extrinsic Stability is caused by the intrusion of air (oxygen and water). The extrinsic degradation can be accelerated by light irradiation. There are organic materials and metal electrodes that are susceptible to degradation caused by oxygen and water. Oxygen or moisture can be trapped during fabrication processes or could diffuse into the cell during device lifetime. OPVs and organic light-emitting diodes (OLEDs) are based on similar materials but are degraded by different mechanisms. In OLEDs, water causes the major extrinsic degradation. Nonetheless, oxygen is dominant in the extrinsic degradation in some OPVs [42] due to the following factors: First, fullerene is hydrophobic and does not react with water. Second, electron-transport properties of fullerene suffer much from the exposure to oxygen in air. Third, oxygen increases the work functions of metals by forming surface dipoles, which deteriorate the performance of conventional OPVs, but may temporarily enhance the performance of inverted OPV [19]. The chemical degradation processes that have been identified are degradation of the metallic electrodes, degradation of the transparent electrode, usually indium tin oxide (ITO), intermediate hole extraction layers (usually PEDOT–PSS) or even the chosen method to synthesize the materials [30, 43]. Oxygen may also constructively affect the electronic properties of other constituent materials in OPVs. Oxygen is

normally a p-type dopant in semiconductors, whereas oxygen vacancies serve as electron donors [44]. Therefore, the electronic properties of the layers in which holes are the majority carrier may temporarily be enhanced upon exposure to oxygen [7]. To overcome this issue, researchers typically fabricate inverted OPVs. The effect of oxygen on the extrinsic degradation of OPVs is less significant than that of water. However, in a humid environment, the thickness of oxide doubles and therefore blocks charge tunneling. Unlike the above mentioned constructive/destructive effects of oxygen, almost no constructive effect of water on OPVs has ever been suggested.

Encapsulation delays the process of degradation, but the currently available materials used for encapsulation do not remove the process. Even if complex encapsulation schemes such as a sealed glass container or a high vacuum chamber are employed, the overall device degradation is not stopped because the processes involving water and oxygen are efficiently alleviated. The physical and chemical characteristics of the constituent materials are a complex phenomenon, in which several processes, both physical and chemical, may take place simultaneously [45].

1.6 Required properties for ideal materials

To design ideal materials for BHJ-OPVs with high PCE following issues need to be carefully addressed.

Open-Circuit Voltage (V_{oc}): generally a minimum energy difference of ~0.3 eV between the LUMO energy levels of the donor compound and the acceptor is required to facilitate efficient exciton splitting and charge dissociation [46].

Short-Circuit Current (J_{sc}): the theoretical upper limit for Jsc of any excitonic solar cell is decided by the number of excitons created during solar illumination. Ideally, the absorption of the active layer should be compatible with the solar spectrum to maximize the exciton generation. Roughly 70% of the sunlight energy is distributed in the wavelength region from 380 to 900 nm [41]; hence, an ideal donor should have a broad and strong absorption in this range, which requires the donor band gap to be 1.4−1.5 eV. A narrower band gap polymer could absorb more light, which would increase the Jsc; however, continuing to lower the band gap would require an increase of the HOMO level of the donor [11] and would reduce the Voc.

Fill factor (FF): that the parallel resistance (R_p) is very large to prevent leakage currents and that the series resistance (R_s) is very low to get a sharp rise in the forward current. The R_s simply adds up from all R_s contributions in the device, that is, from bulk transport, from interface transfer and from transport through the contacts. The R_s and R_p are significantly impacted by the morphology of the polymer/fullerene blend and R_p also on the contact quality surface in between electrodes (Figure 1.6(a)).

The characteristic influence of these resistivity is shown in Fig. 1.6(b). Thus, the morphology of the active layer should be optimized to promote charge separation and favorable transport of the photogenerated charges in order to maximize the FF and the attainable J_{sc} [46].

Finally, besides high PCE, solution processability and long-term stability of OPV (related with both materials and encapsulation) are of equal importance for future application and commercialization [11].

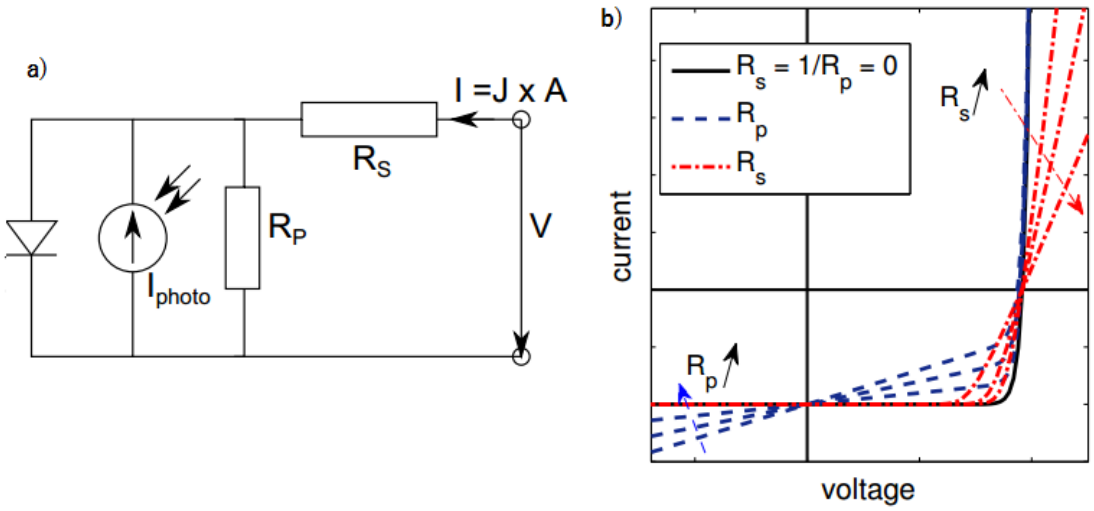

Figure 1.6: (a) Simple equivalent circuit of a solar cell. It contains a diode, a photocurrent source and R_p and R_s. (b) Influence of series resistance R_s and parallel resistance R_p, mainly changing the fill factor.

1.7 Design of OPVs Devices

The BHJ (bulk heterojunction) structure for OPVs is shown in Figure 1.3 Although thermal co-deposition methods can be used to fabricate a BHJ, the junction is y formed by intermixing donor and acceptor materials in a solution, then forming the active layer by spin coating of the mixed solution on a substrate.

After the electrical charge carriers move to the active layer/electrode interface, they are extracted from the active layer to the electrodes. To achieve high efficiency in charge extraction, the potential barrier at the active layer/electrode interfaces have to be minimized. Thus, the work function (WF) of

the anode is ideally expected to match the donor HOMO, while the work function of the cathode is expected to match the acceptor LUMO. When these features occur, the contacts are called ohmic contacts and Voc correlates positively with the difference between the acceptor LUMO and donor HOMO. Normally Al or Ag is used as metal electrode. The WF of Al is from 4.06 eV to 4.26 eV and Ag is from 4.26 eV to 4.74 eV. Commonly, indium tin oxide (ITO) is used as an anode with a WF from 4.7 eV to 4.1 eV.

The active film is an interpenetrating nanoscale network of donor and acceptor materials. The phase separation within the film should be commonly 10–20 nm, which is within the exciton diffusion length of many organic semiconductors. Consequently, nearly unity internal quantum efficiency has been achieved for BHJ solar cell, which means that nearly all photogenerated excitons are dissociated [47].

Charge carriers are then transported through percolated pathways within the active layer toward the respective contacts for collection. Due to the small nanoscale phase separation in BHJs, a thicker active layer can be fabricated in these cells when compared to bilayer solar cells. However, as the spin-coating process is inherently less controlled than the vapor deposition process commonly used in bilayer solar cells, the performance of BHJ solar cells is susceptible to various parameters. The efficiency of solar cells is strongly dependent on the morphology of the BHJ and various treated methods such as thermal annealing, solvent annealing, and modifying polymer functional groups have been studied to optimize the OPVs performance [18].

Chapter 2

Experimental Development

This chapter describes in detail the structure of the OPVs and characteristics that materials must comply as well as the main features of the used adhesives and two ways to encapsulate devices.

2.1 Materials and sample preparation of OPVs

In this work, the used materials were the conjugated polymers poly(3-hexylthiophene-2,5-diyl) (P3HT) as electron donor material and the fullerene

derivative [6,6]-phenyl C71 butyric acid methyl ester ($PC_{71}BM$) as the electron acceptor for the active layer. P3HT polymer is used as it is more stable than others, for example MDMO-PPV and thieno(3,4-b)-thiophene/benzodithiophene copolymer and [6,6]-phenyl C71 butyric acid methyl ester (PTB7:PC71BM) [31, 49]. Solvents and reagents were used without further purification process. The polymer poly(3,4-ethyl-enedioxythiophene)-poly(styrenesulfonate) (PEDOT:PSS) is used as hole transport layer (HTL) and the alcohol/water-soluble conjugated polymer poly [(9,9-bis(30-(N,N-dimethylamino) propyl)-2,7-fluorene)-alt-2,7-(9,9-dioctylfluorene)] (PFN) as an electron transport layer (ETL). It was used ITO/glass substrates with 4–10 Ω/square and the use of the eutectic mix of FM (32.5% Bi, 51% In, 16.5% Sn) with a meling point obove 62 °C [50, 51] as cathode, fabrication of the OPVs was easy and fast, without the need of a vacuum step. Figure 2.1 shows the chemical molecular structure of the mentioned organic materials.

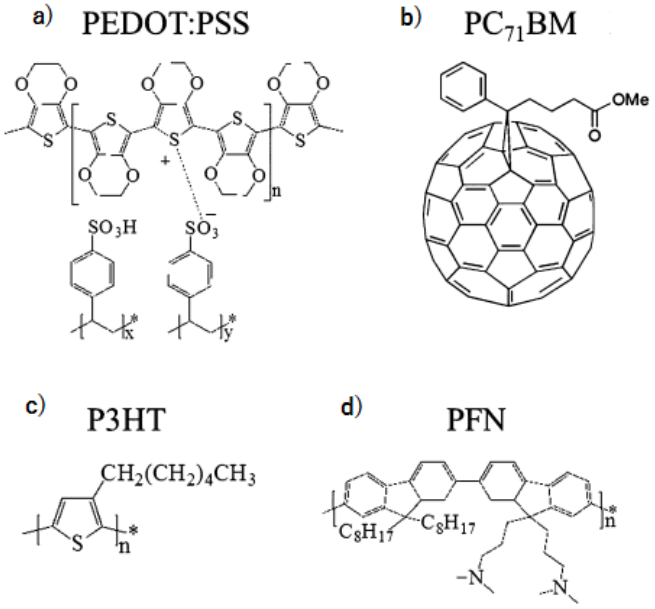

Figure 2.1 Chemical structures of the organic used compounds a) as hole transport layer (PEDOT:PSS), b) as electron acceptor ($PC_{71}BM$), c) as electron donor material (P3HT) and d) as an electron transport layer (PFN).

The solar cells based on P3HT:$PC_{71}BM$ were fabricated using a common process under ambient conditions. Prior to device fabrication, the indium tin oxide (ITO) coated glass substrates were sequentially cleaned in detergent, de-ionized water, acetone and isopropanol and treated with oxygen plasma for 5 min. The hole-injection buffer layer of PEDOT:PSS was spin-coated on the ITO-coated glass substrate at 4000 RPM for 45s (40 nm of thickness), the PEDOT:PSS-coated substrates were thermally treated for 15 min at 100 °C in a hot plate. The P3HT:$PC_{71}BM$ mixture (1:0.8 w/w) was dissolved in dichlorobenzene and stirred for 12h at 0 °C under normal conditions. This solution was spin coated onto PEDOT:PSS coated substrates (1800 rpm, 100 nm of thickness). Then, this film was subjected to thermal annealing for 15min at 100 °C. The PFN interlayer material was dissolved in methanol (concentration: 2mg/ml) under the presence of a small amount of acetic acid (10 µl) to prepare 5 ml of a standard solution. The resulting mixture was diluted with methanol (1:5 v/v) and spin-coated at 6000 RPM for 45s (10nm of thickness) on top of active layer. Finally, Field's metal pellets were melted on a hotplate at 85 °C. The melted eutectic alloy was deposited drop-wise on the patterned substrate, the active area was 0.04 cm^2. Figure 2.2 a) shows the configuration of the fabricated OPVs. Figure 2.2 b) shows the energy levels for the devices. According to the energy levels of $PC_{71}BM$ and P3HT, the isolated $PC_{71}BM$ aggregations in the blend films can be considered as electron traps due to the energy barrier of 1.3 eV between the LUMOs of P3HT.

The barriers for electron from ITO onto the lowest unoccupied molecular orbital (LUMO) of P3HT and $PC_{71}BM$ are 1.5 eV and 1.1 eV, respectively [28].

Meanwhile, the barriers for hole collection from FM (4.47 eV) onto the highest occupied molecular orbital (HOMO) of P3HT and $PC_{71}BM$ are, 0.8 eV and 1.6 eV, respectively. [43]

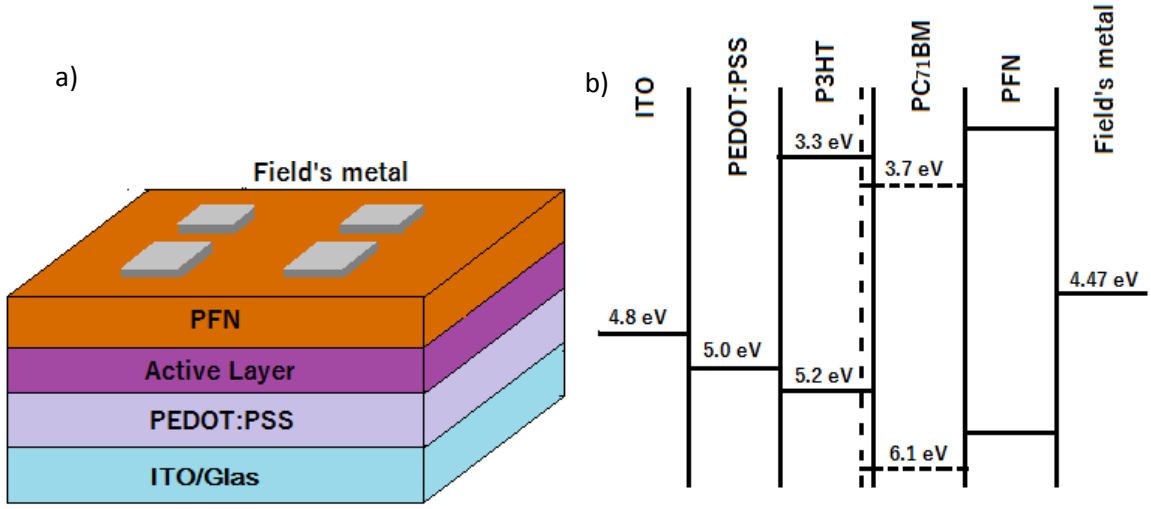

Figure 2.2 a) Schematic architecture of the devices based on P3HT:$PC_{71}BM$ as active layer. b) Schematic diagram of the energy levels for the fabricated devices.

Finally OPVs devices were tested using a Keithley Source Meter 2400 and a halogen lamp. Light intensity was calibrated to 100 mW/cm^2 (AM1.5 conditions) using an Oriel reference cell. Data were acquired by a LabVIEW software specially designed for this purpose.

2.2 Used Materials for Encapsulation of OPVs Devices

For the device encapsulation, UV-curable polymers (Norland Optical Adhesives: NOA) were used to encapsulate the organic solar cells devices (OPVs) [8]. These adhesives can provide excellent light transmission over a wide spectral range; have low strain and good optical clarity unlike other reported encapsulants [29-39]. These adhesives do not require premixing operations, they do not need any vacuum process to use them as encapsulants neither thermal curing, which may result in a more rapid degradation of the devices [7]. For OPVs uses, for instance, in Ref. [39] the adhesive NOA 91 was used to encapsulate the OPVs devices with the ITO/PEDOT:PSS/PTB7:PC71BM/TiOx/Al structure by employing sealant glass; this adhesive was chosen because of its optical characteristics and curing with UV light without the need for a subsequent heat treatment. The Norland adhesives have advantages in bonding applications that require optical clarity or require fast curing times and long term stability over a wide range of temperatures. These adhesives are applied in different areas such as artwork for gemstone filling, gemstone bonding and glass dresses, in fiber optics for coating high-index fiber, in holograms for design and fabrication of a high-density 2D fiber array for holographic switching applications, holographic recording and lighting, among others [41-53]. For OPVs uses, for instance, in Ref. [39] the adhesive NOA 91 was used to encapsulate the OPVs devices with the ITO/PEDOT:PSS/PTB7:PC71BM/TiOx/Al structure by employing sealant glass; this adhesive was chosen because of its optical characteristics and curing with UV light without the need for a subsequent heat treatment.

In this work five NOA adhesives were used: 61, 65, 71, 76 and 123; Table 2.1 shows some general properties. NOA curing time is remarkably fast (5-10 s with a Opticure LED has a UV energy output at full power of 2.5 W/cm^2 at 365nm), and it is dependent upon the ultraviolet light energy available. The characteristics of these adhesives are [8]:

Table 2.1 Properties of the Norland adhesives.

NOA	61	65	71	76	123
Refractive Index of Cured Polymer	1.56	1.524	1.56	1.51	1.52
Elongation at Failure	38%	80%	43%	47%	60%
Modulus of Elasticity (psi)	150,000	20,000	55,000	970	50,000
Tensile Strength (psi)	3,000	1,500	1,300	450	3,000
Water Absorption	16%	16%	16%	16%	16%

NOA 61: The adhesive is designed to give the best possible optical bond to glass surfaces, metals, fiberglass and glass filled plastics, it has excellent clarity, low shrinkage and flexibility. These characteristics are important in order to produce high quality optics and achieve long term performance under changing environments. It is cured by ultraviolet light with maximum absorption UV within the range of 320-380 nm with peak sensitivity around 365nm. When fully cured, it has very good adhesion and solvent resistance, however, without reaching its optimum adhesion to glass.

NOA 65: The cured adhesive is very flexible and was designed to minimize strain. It is especially suitable where the adhesive cross section would be relatively thick, has enough elasticity to keep strain to a minimum even when materials with different coefficients of expansion are bonded together. NOA 65 is cured by ultraviolet light with a maximum absorption UV within the range of 350-380 nm. The polymer has minimum oxygen

inhibition, and therefore any surface in contact with air will be non-tacky when fully cured.

NOA 71: This adhesive can also be used for adhering to other substrates, such as metal, fiber- glass, and glass filled plastics. Typical applications are, holographic plates, flat panel displays and touch screens or as a clear coating on plastic or metal. When fully cured provides strong adhesion to glass surfaces. It is cured with long wavelength UV light from 315 to 400 nm with peak absorption at 365 nm. Since the beginning of curing exposure to UV light is desirable to achieve a minimum of stress and tension. When fully cured, it has very good adhesion and solvent resistance. The best adhesion and extra strength will reached after 1 week at room temperature. The NOA 71 has an adhesion promoter in it that provides maximum adhesion and moisture resistance when used in glass, glass-filled or ceramic bonding applications.

NOA 76: It is recommended for bonding glass to plastic. The adhesive has best adhesion with plastics such as acrylic, polycarbonate and cellulose acetate butyrate with typical applications being glass to plastic bonding or laminating polarized film between glass. NOA 76 is cured by ultraviolet light between 315 to 400 nm and visible light between 400 to 450 nm. The peak absorption wavelengths are 325, 365 and 400 nm. Minor absorption wavelengths are 410, 420 and 450 nm.

NOA 123: It is used to form a bridge between the component and the substrate; it has very good adhesion to glass, metals, printed circuit boards and many plastics. The unique disadvantage of these adhesives is that even though they cure in seconds, they are extremely stable when not exposed to ultraviolet light. It is sensitive to the whole range of UV light from 320 to

380 nm with peak sensitivity around 365 nm. It contains a latent heat catalyst that can quickly cure areas that do not receive the ultraviolet light. The catalyst allows the adhesive to cure in 10 minutes at 125° C in a convection oven, or 3 hours at 80° C. Since the cure is very exothermic, the adhesive should be allowed to cool back to room temperature.

2.3 Encapsulation ways in OPVs devices

The encapsulation of the OPVs were performed in two different ways, the first one is the traditional glass cap encapsulation (GCE) device, using each of the adhesives Norland to glue glass cap and substrate together (Figure 2.6.a) and the second is applying the adhesive directly onto the device (Figure 2.6.b). With NOA 123, because of its very liquid consistency, it was used for the direct encapsulation of the device.

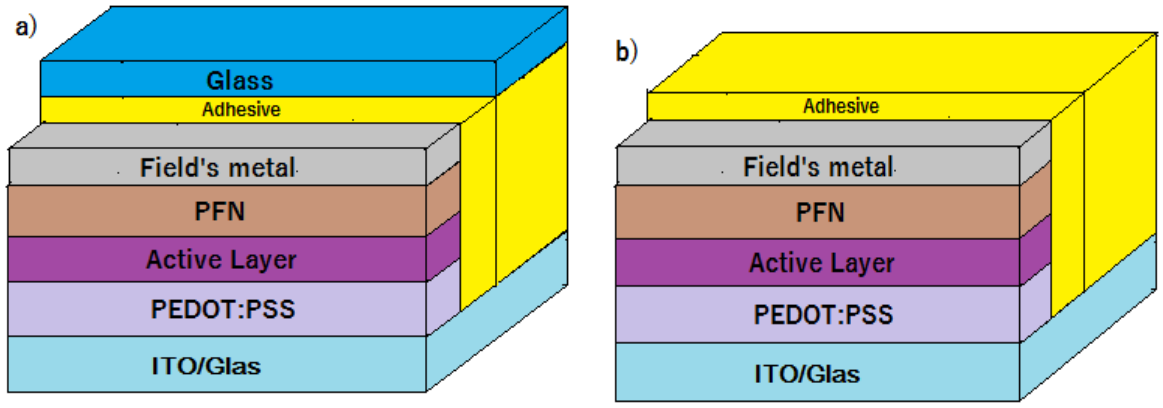

Figure 2.6 A schematic diagram of encapsulated ITO/PEDOT:PSS/P3HT:PC71BM/Field's metal devices, a) GCE way and b) applying the adhesive directly

Further, devices were encapsulated under two different atmospheres: a) inside of a glove box system under nitrogen (N_2) ambient and b) under normal room conditions. The used UV lamp to cure the adhesives was a high-pressure mercury (Hg) lamp (exposed light intensity of 50 mW/cm^2 at 370 nm). OPVs devices were irradiated at a distance of 2 cm with an intensity of 4 mW/cm^2, which was measured with a thermopile. The time of curing adhesives is different; these periods are shown in Table 2.2.

Table 2.2 Curing time for each used Norland adhesive by employing a high-pressure mercury (Hg) light lamp with an intensity about 4 mW/cm^2.

NOA Adhesive	Time(s)
61	2
65	3
71	5
76	4
123	1

OPVs cells were measured before and after being encapsulated. All devices were kept exposed to minimal room light and measured under normal conditions, i.e. outside glove box.

Chapter 3

Results and Discussion

In this thesis OPVs devices were encapsulated in two atmospheres: inside glove box (N_2 atmosphere) and under normal conditions. This chapter shows how exposure of UV light affects the active layer of the devices by observing its absorption spectra and by acquiring AFM images. Also here it is presented the performance over time of the encapsulated OPVs with the two methods and under different atmospheres; it is to determine the best used adhesive and conditions. The encapsulated OPVs by using the Norland adhesives achieved longer lifetime

under N_2 atmosphere. The encapsulated cells were kept with minimal lighting and frequently monitored until their efficiencies were down to only 20% (%) or well broke down.

3.1 Absorption spectra and AFM images

Firstly, it was observed the effect on the absorption coefficient from three films (P3HT, $PC_{71}BM$ and P3HT:$PC_{71}BM$) each with different times of exposure to UV light (5s, 30s and 1 minute). The broad absorption peaks in the range from 350 to 500 nm are due to absorption of $PC_{71}BM$ [53]. Figure 3.1.a shows absorption coefficient of P3HT and Figure 3.2.b for $PC_{71}BM$ respectively. The absorption coefficient of the P3HT:$PC_{71}BM$ is shown in Fig. 3.1.c. The blend film shows a broad spectral absorption ranging from 450 to 650 nm as reported in [55].

a)

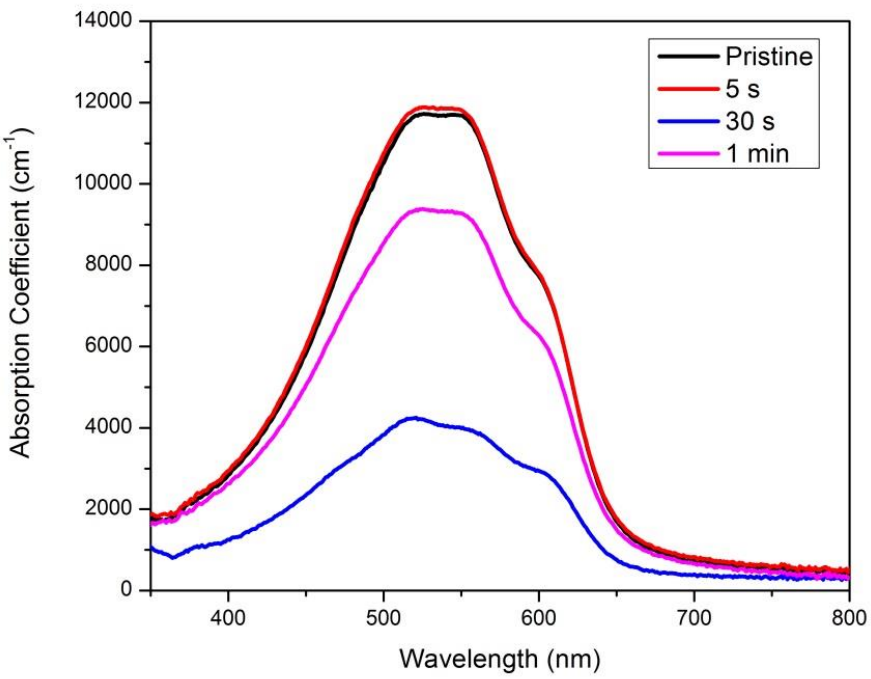
Pristine
5 s
30 s
1 min
Absorption Coefficient (cm-1)
Wavelength (nm)
0
2000
4000
6000
8000
10000
12000
14000
400
500
600
700
800

b)

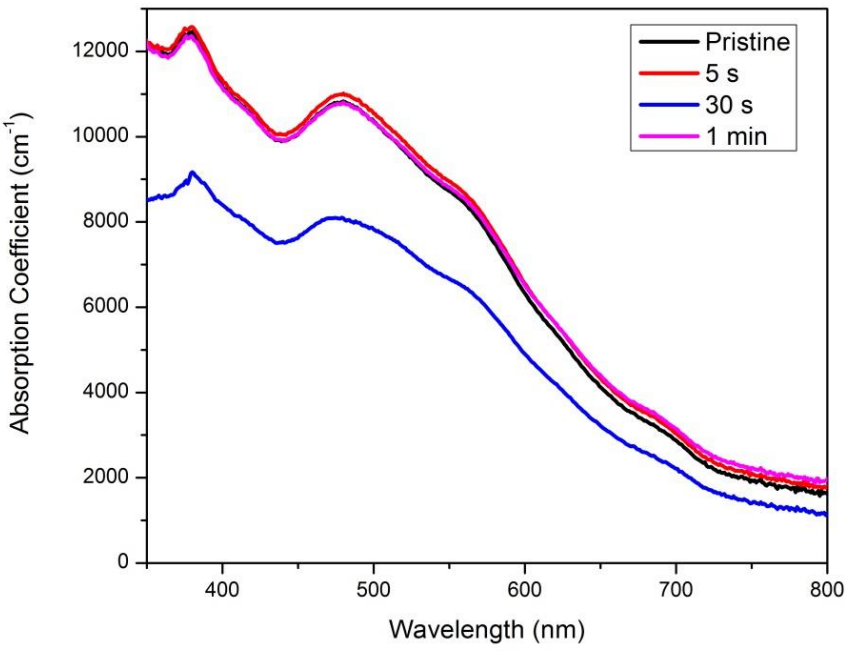
Pristine
5 s
30 s
1 min
Absorption Coefficient (cm-1)
Wavelength (nm)
0
2000
4000
6000
8000
10000
12000
400
500
600
700
800

c)

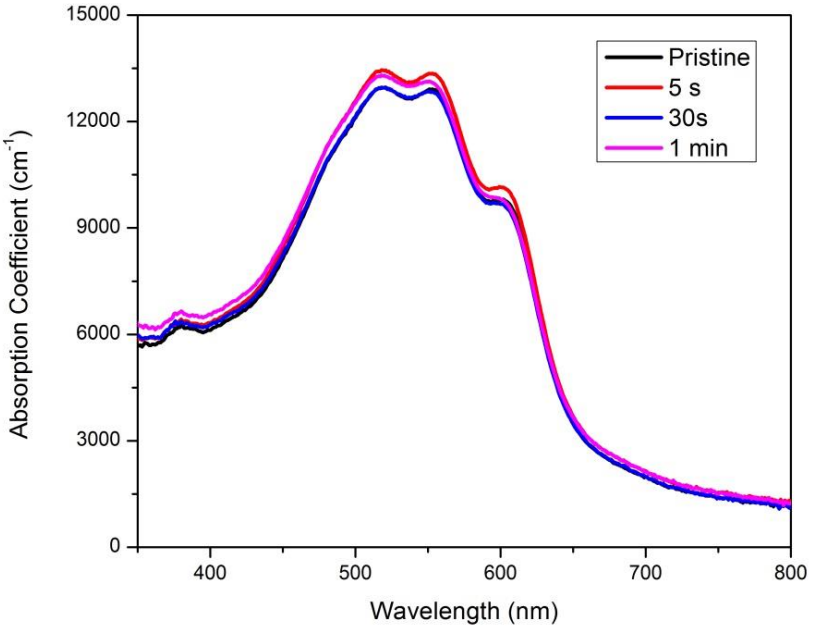

Figure 3.1. Absorption coefficient spectra from three films with different exposure times to UV light a) P3HT, b) $PC_{71}BM$ and c) P3HT:$PC_{71}BM$

For the films of P3HT:$PC_{71}BM$ and $PC_{71}BM$ the absorption peaks decreased drastically after 30 s exposed to UV light but after a minute the absorption peak increases again, but does not return to its original state. This phenomenon does not occur in the film P3HT.

Figure 3.2 shows the comparison of AFM images for P3HT:$PC_{71}BM$ blends before/after being exposed to UV-light. Fig. 3.2.a is the pristine film and Fig. 3.2.b shows the film after 5s of exposure to UV-light. The films have slightly changed surface morphologies after 30 seconds (Figure 3.2.c) after exposure to UV light. However the change in the morphology of the film after one minute (Figure 3.2.d) of exposure to UV light is much more dramatic, i.e. to longer exposition to UV-light,

larger morphological changes are observed. According to literature [37, 38] the exposing the film TO UV-light does not affect the efficiency of the device. The OPV encapsulated with NOA 71 is the most time is exposition to UV-light (5s).

a)

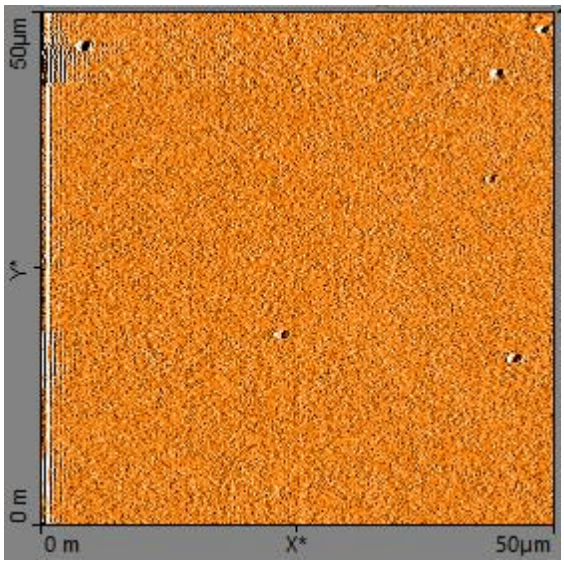

b)

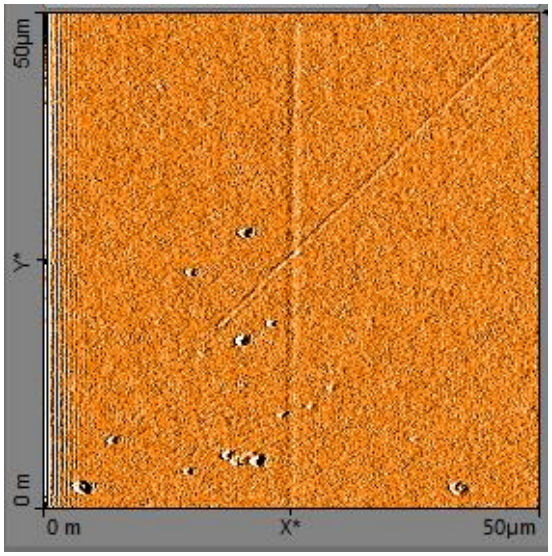

c)

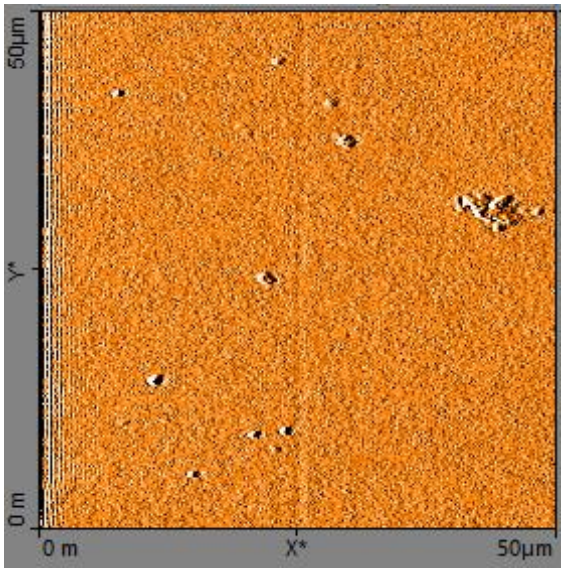

d)

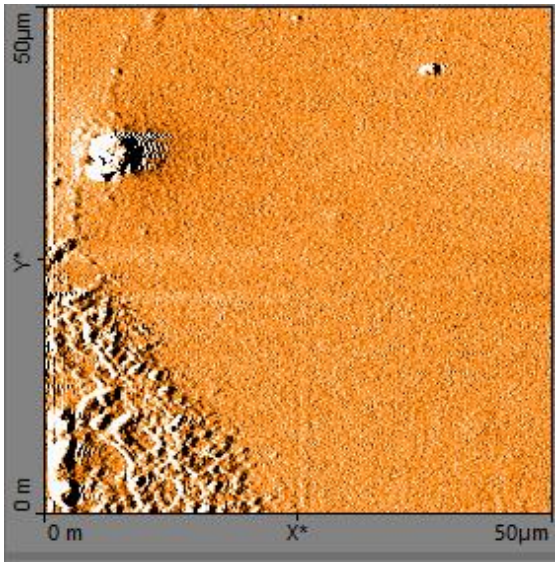

Figure 3.2. AFM images of the (a) P3HT:$PC_{71}BM$ (pristine), (b) P3HT:PC71BM (after 5 seconds), (c) P3HT:$PC_{71}BM$ (after 30 seconds), and (d) P3HT:$PC_{71}BM$ (after 1 minute).

3.2 OPVs devices encapsulated outside glovebox

In Figure 3.3.a) curves are shown for the initial current density–voltage (J–V) characteristics for all cells without encapsulation and Figure 3.3.b) shows the characteristics for curves J–V for all devices after being encapsulated. All OPVs devices were encapsulated and measured immediately; using the NOA adhesives and the ways described in sections 2.2 and 2.3 respectively.

The devices were monitored a total of 46 days before starting to fail. In this case the degradation of J_{sc} shows an irregular behavior probably due to the water and oxygen that are still present within the cell. The latter makes sense because the cells were not encapsulated in a controlled environment and therefore the penetration of oxygen and water is much more likely that the cells encapsulated within glove box. Parameters were plotted separately for each of the encapsulation performed methods.

Figure 3.4 shows a voltage variation over 46 days (1104 hours), in the case of direct encapsulation, it decreased only 3% using NOA 71, while with the GCE method decreased 5% using NOA 65, In the case of current density (Figure 3.5), it

decreased 18% for the direcencapsulated cell and 35% with the GCE method in both cases with NOA 65. For the FF (Figure 3.6), it decreased 28% for the directway and 36% for GDE method in both cases with NOA 71 Finally PCE (Figure 3.7) decreased 27% for direct encapsulation applied with NOA 71 and 50% using the GCE method with the adhesive NOA 65. Table 3.1 shows degradation parameters for each OPVs encapsulated procedure with different adhesives.

a) without encapsulation

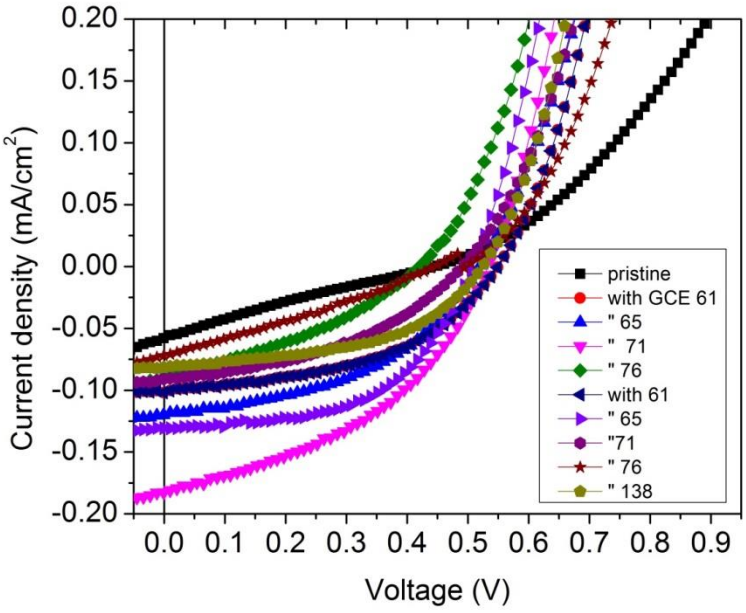

b) with encapsulation

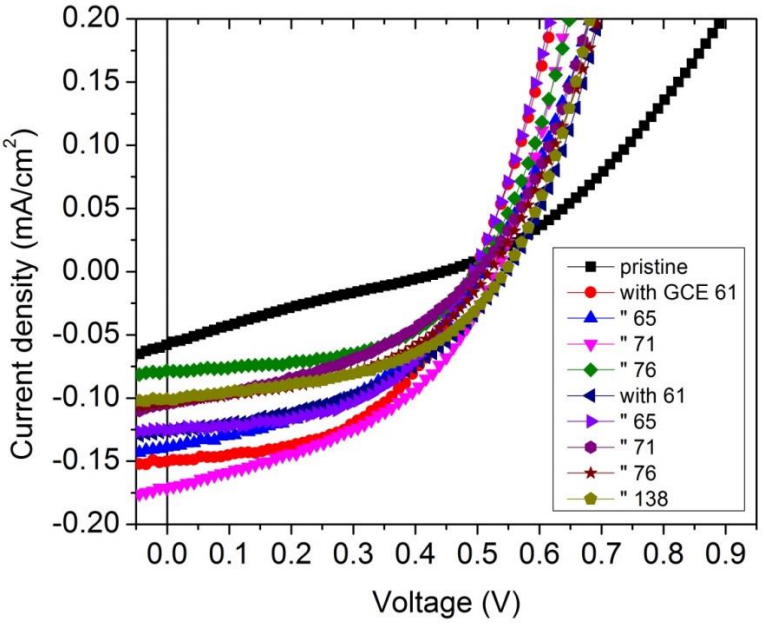

Figure 3.3. Initial *J*–*V* characteristics under illumination of AM 1.5 G, 100 mW/cm^2, for a) all OPVs before being encapsulated and b) all OPVs devices encapsulating outside glovebox. Cells configuration: ITO/PEDOT:PSS/P3HT:$PC_{71}BM$/FM

a)

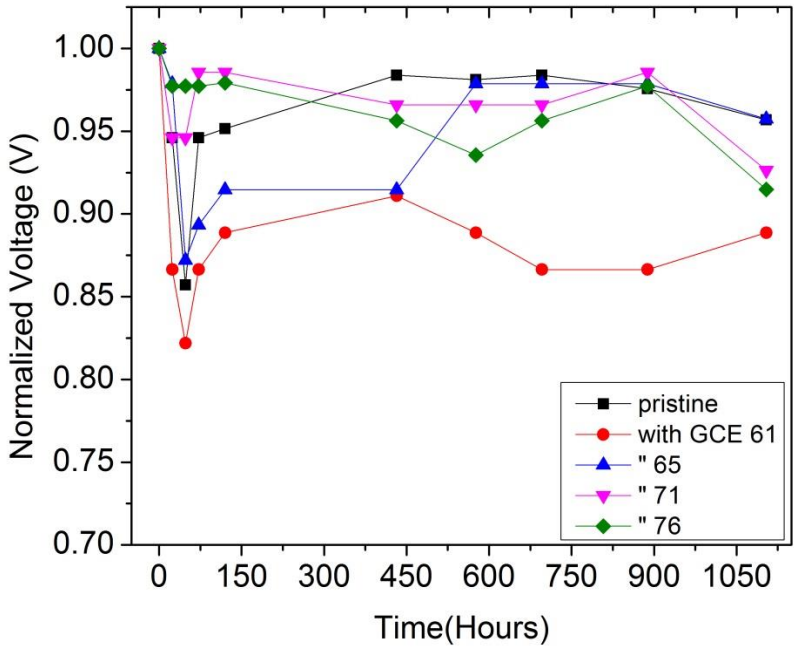

b)

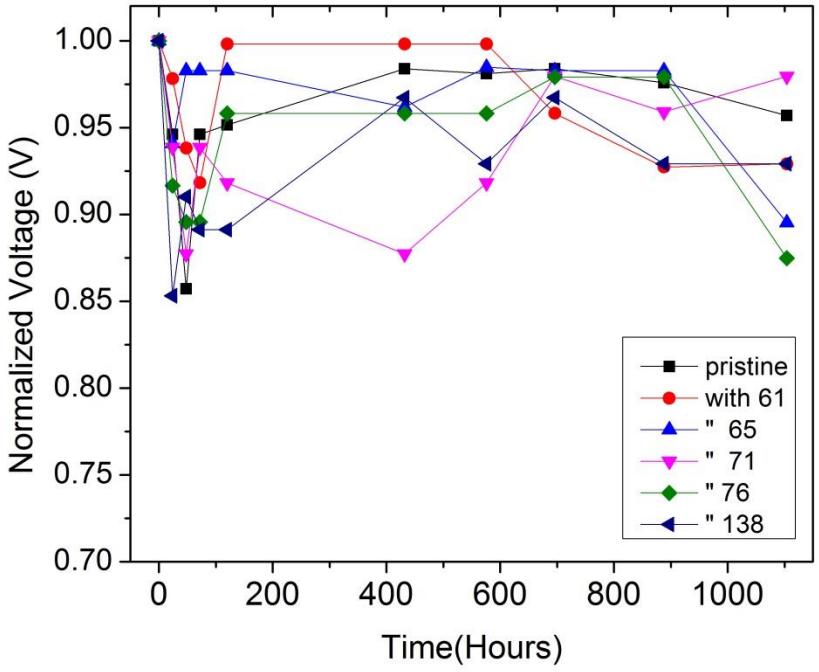

Figure 3.4. Normalized voltage variation as a function of time for OPV devices ITO/PEDOT:PSS/P3HT:PCBM/FM encapsulated with Norland adhesives (61,65,71,76 and 138) outside a glove box a) covered with a glass plate and sealed and b) applying the adhesive directly on the cell. In both cases, adhesives were exposed to UV light.

a)

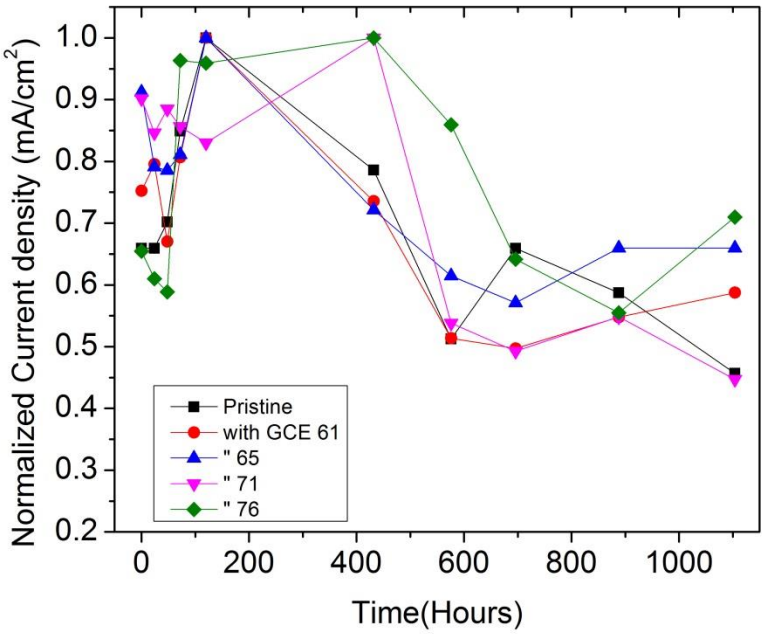

b)

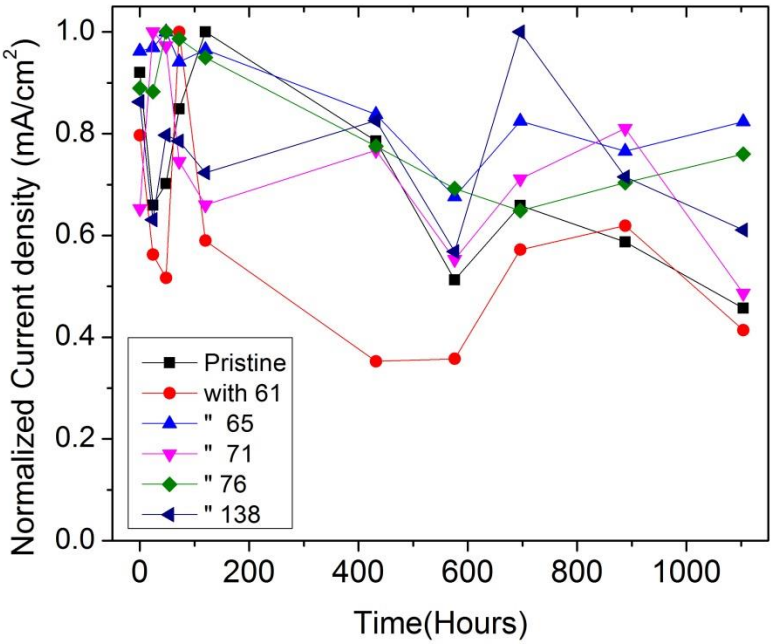

Figure 3.5. Normalized current density variation as a function of time for OPV devices ITO/PEDOT:PSS/P3HT:PCBM/FM encapsulated with Norland adhesives (61,62,71,76 and 138) outside a glove box a) covered with a glass plate and sealed and b) applying the adhesive directly on the cell. In both cases, adhesives were exposed to UV light.

a)

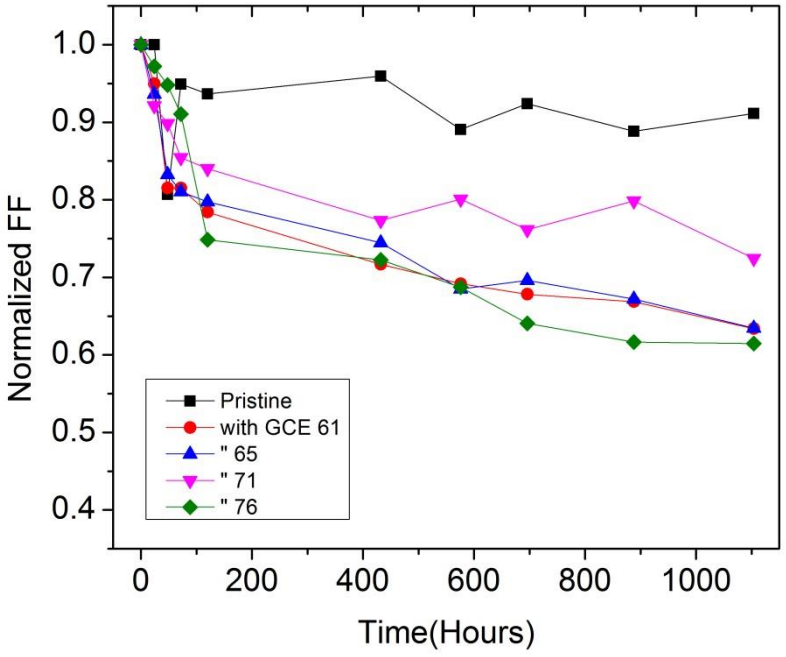

b)

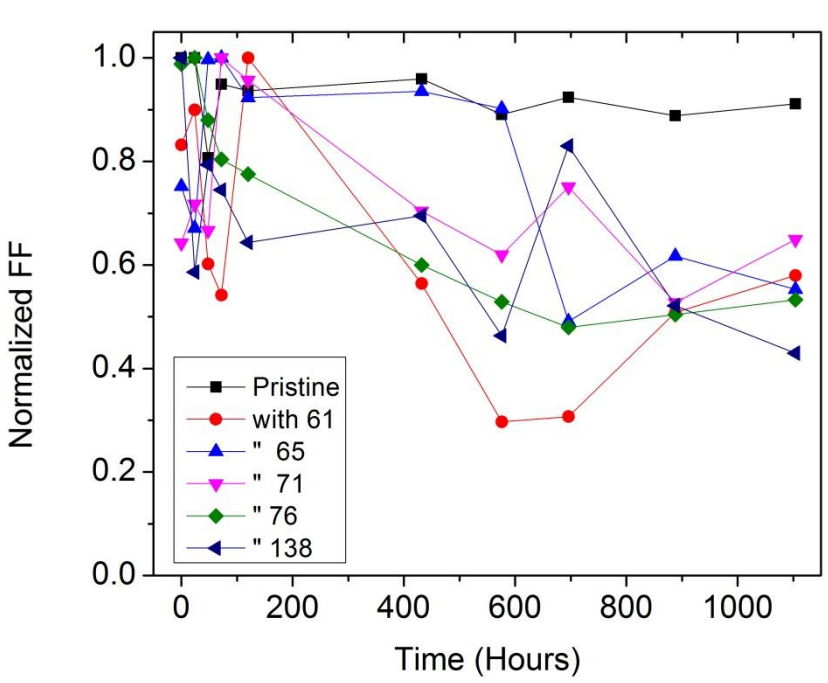

Figure 3.6. Normalized FF variation as a function of time for OPV devices ITO/PEDOT:PSS/P3HT:PCBM/FM encapsulated with Norland adhesives (61,62,71,76 and 138) outside a glove box a) covered with a glass plate and sealed and b) applying the adhesive directly on the cell. In both cases, adhesives were exposed to UV light.

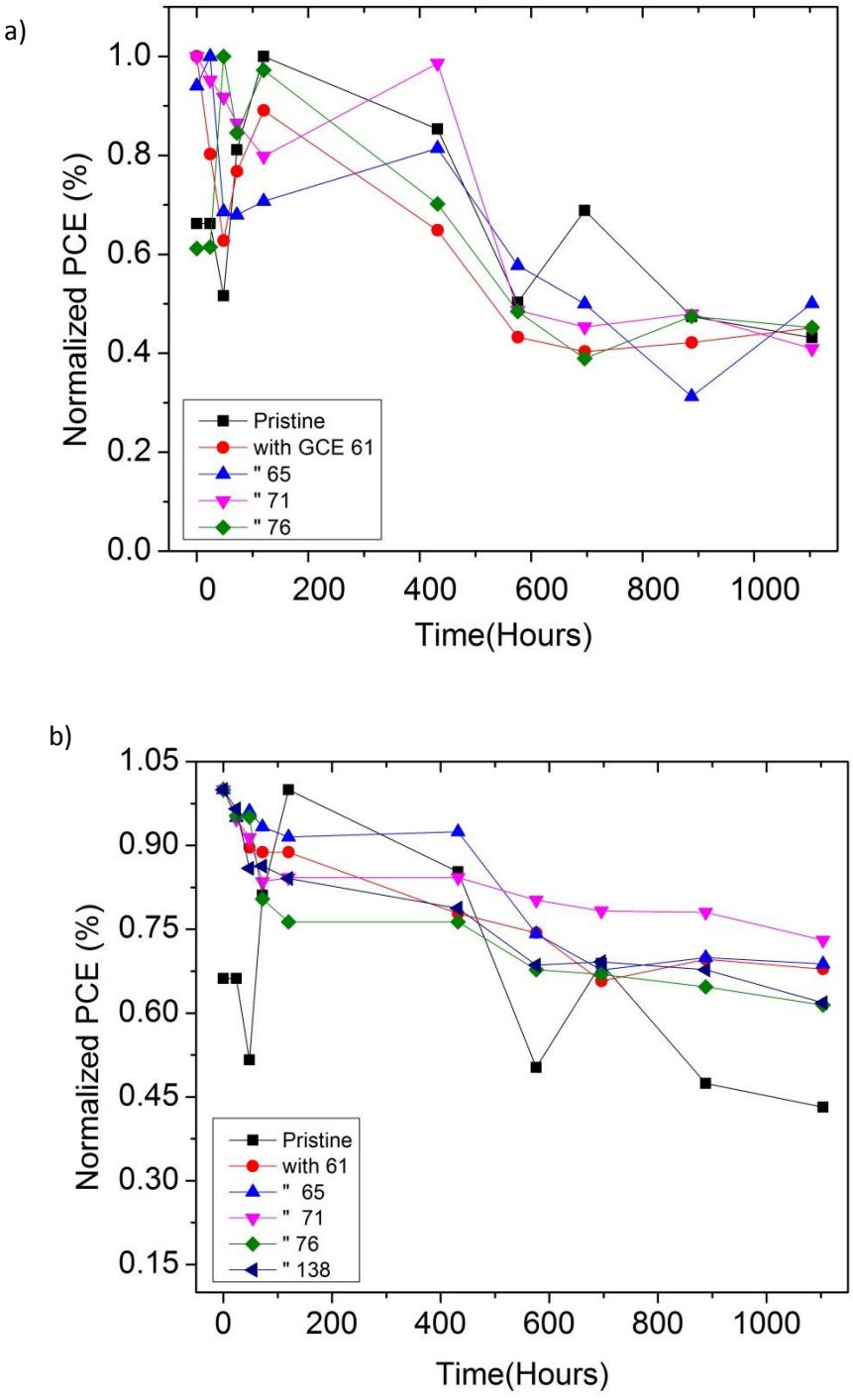

Figure 3.7. Normalized PCE variation as a function of time for OPV devices ITO/PEDOT:PSS/P3HT:PCBM/FM encapsulated with Norland adhesives (61,62,71,76 and 138) outside a glove box a) covered with a glass plate and sealed and b) applying the adhesive directly on the cell. In both cases, adhesives were exposed to UV light.

Table 3.1. Percentage of decay after 46 days of monitoring encapsulated OPVs devices (under normal room conditions) for the PV parameters: voltage, current density, FF and PCE, by using both, the direct and GCE procedures.

Procedures	Voltage	Current density	FF	PCE
GCE method	5%/NOA 65	30%/NOA 76	28%/NOA 71	50%/NOA 65
Direct	3%/NOA 71	18%/NOA 65	36%/NOA 71	27%/NOA 71
Pistine	5%	45%	9%	64%

OPVs that degrade in less degree were those encapsulated with the adhesives NOA 65 and NOA 71 using the GCE method and applying the adhesive directly, respectively. Furthermore, some of the encapsulated cells with the direct way, degraded less than OPVs encapsulated with the GCE method. In Figure 3.8. can be seen the efficiency degradation of the best encapsulated OPVs, with NOA 65 and the GCE method preserve a 50 % of efficiency, while the OPVs encapsulated with NOA 71 and directly preserve a 73%.

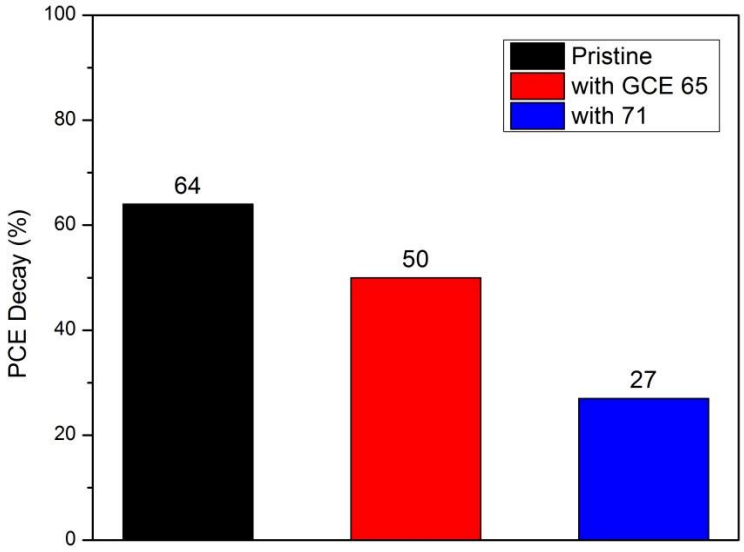

Figure 3.8. Efficiency of the OPVs encapsulated outside glovebox that degrade less after 46 days.

Regarding literature, Ref [30] reports a cell with the structure ITO/ZnO/P3HT:PCBM/PEDOT:PSS/Al, where all layers were deposited under a N_2 filled glove box, but encapsulated under normal condition. They used ZnO as buffer layer and UV resin solution for encapsulation. ZnO layer is spin-coated on top of a solar cell. For encapsulation, UV resin solution was dropped on top of ZnO layer and later on annealed at 120°C for 20 min. It was carried out under normal conditions and applying the resin directly on the cell. The power conversion efficiency (PCE) degrades by 20.5% after 672 h (28 days) in air. In this thesis the encapsulated OPVs with Norland adhesives, with the determined best lifetime, were by using NOA 65 and NOA 71. They degraded 20% with GCE method after 432 h and 888 h directly, respectively.

3.3 OPVs devices encapsulated inside a glove box (Under N_2 atmosphere)

Figure 3.9.a) shows the characteristics curves for the initial current density–voltage (J–V) for all cells without encapsulation and Figure 3.9.b) shows the characteristics curves J–V for cells after some minutes of being encapsulated. The devices were monitored for a total of 57 days before to fail. In this case the cells were prepared under normal conditions and encapsulated in a controlled environment (N_2 atmosphere) and therefore the penetration of oxygen and water is much lower than the cells encapsulated outside glove box. In this case, OPVs cells worked 9 days more than OPVs encapsulated outside glove box.

a) With encapsulation

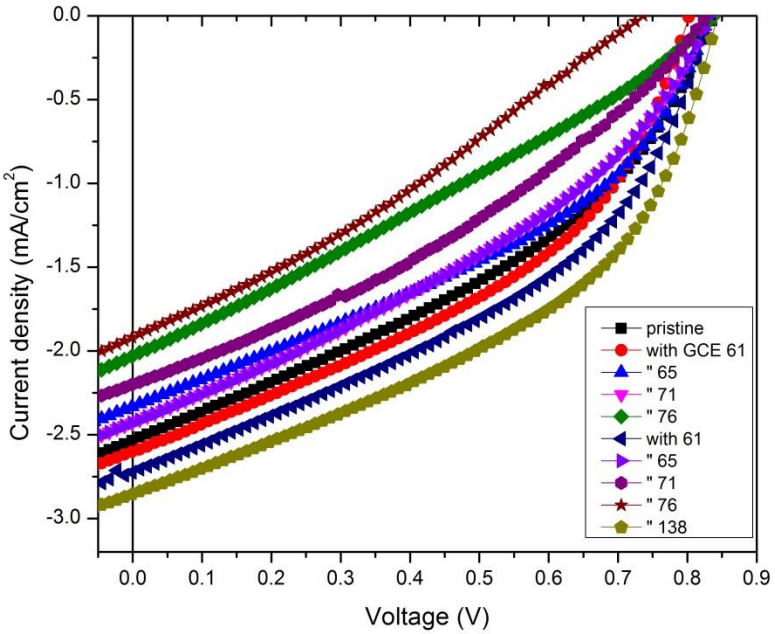

b) Within encapsulation

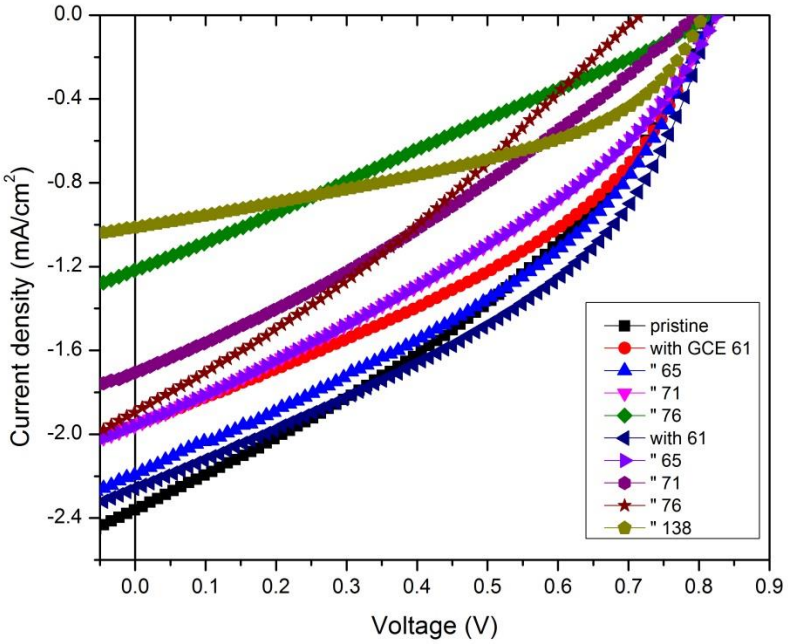

Figure 3.9. Initial *J*–*V* characteristics under illumination of AM 1.5 G, 100 mW/cm^2, for a) all OPVs before being encapsulated and b) all OPVs devices encapsulating inside a glovebox. Cells configuration: ITO/PEDOT:PSS/P3HT:PC_{71}BM/FM

Figure 3.10 shows a voltage variation over 57 days in the case of direct encapsulation, it decreased 2% using NOA 76, while with the GCE method decreased 10% using NOA 71. In the case of the short circuit current density (Figure 3.11), decreased 55% for the direct encapsulated cell with NOA 76 and, just 42% with the GCE method using NOA 71. For the FF (Figure 3.12) it decreased 11% for direct way of encapsulation using NOA 71, for GCE method decreased 30% using NOA 76. Finally PCE (Figure 3.13) decreased 33% for direct encapsulation with NOA 71, with the GCE method decreased 32% with NOA 65. Tables 3.2 show degradation parameters for each OPVs encapsulated by using both of the mentioned ways inside a glove box (under N_2 atmosphere) after 57 days with different adhesives.

a)

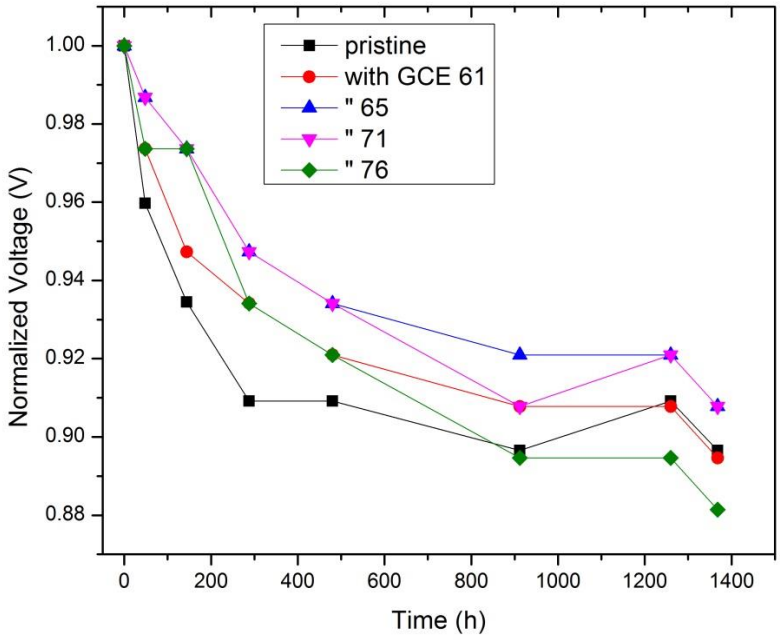

b)

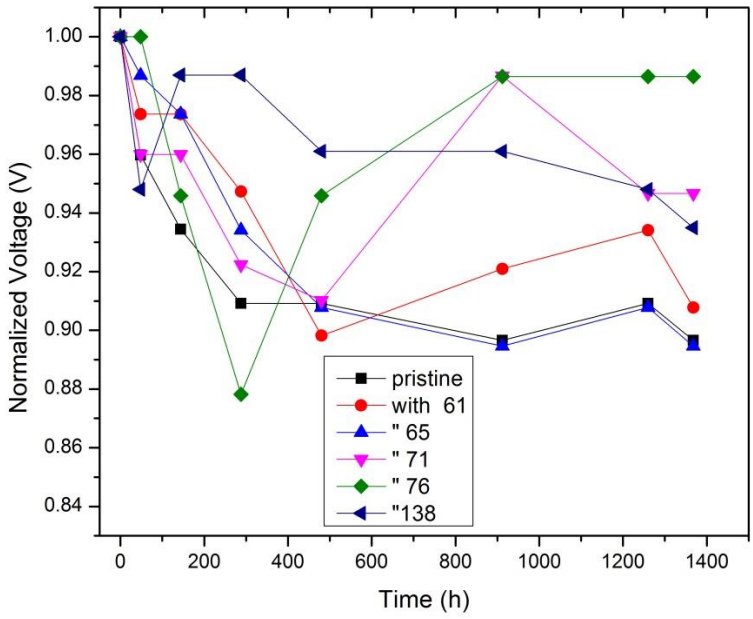

Figure 3.10. Normalized voltage variation as a function of time for OPV devices ITO/PEDOT:PSS/P3HT:PCBM/FM encapsulated with Norland adhesives (61,62,71,76 and 138) inside a glove box a) covered with a glass plate and sealed and b) applying the adhesive directly on the cell. In both cases, adhesives were exposed to UV light.

a)

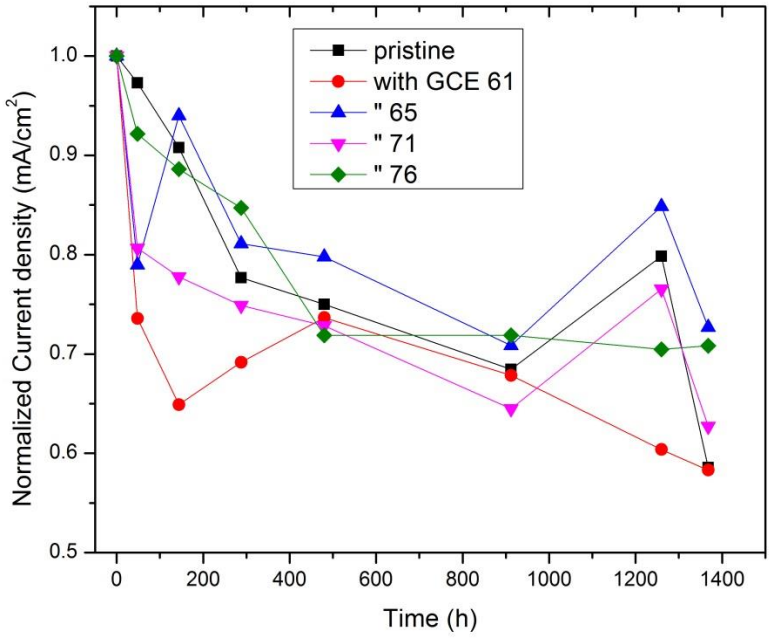

b)

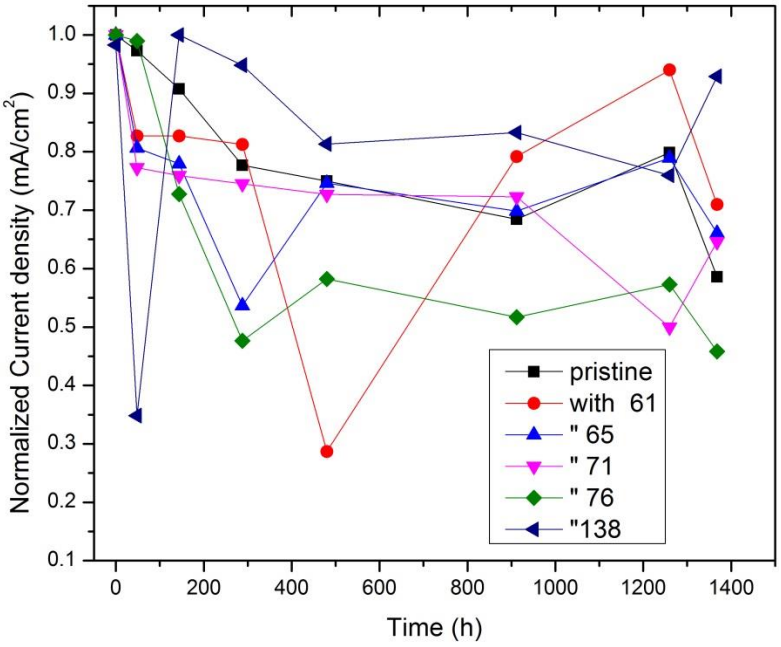

Figure 3.11. Normalized current density variation as a function of time for OPV devices ITO/PEDOT:PSS/P3HT:PCBM/FM encapsulated with Norland adhesives (61,62,71,76 and 138) inside a glove box a) covered with a glass plate and sealed and b) applying the adhesive directly on the cell. In both cases, adhesives were exposed to UV light.

a)

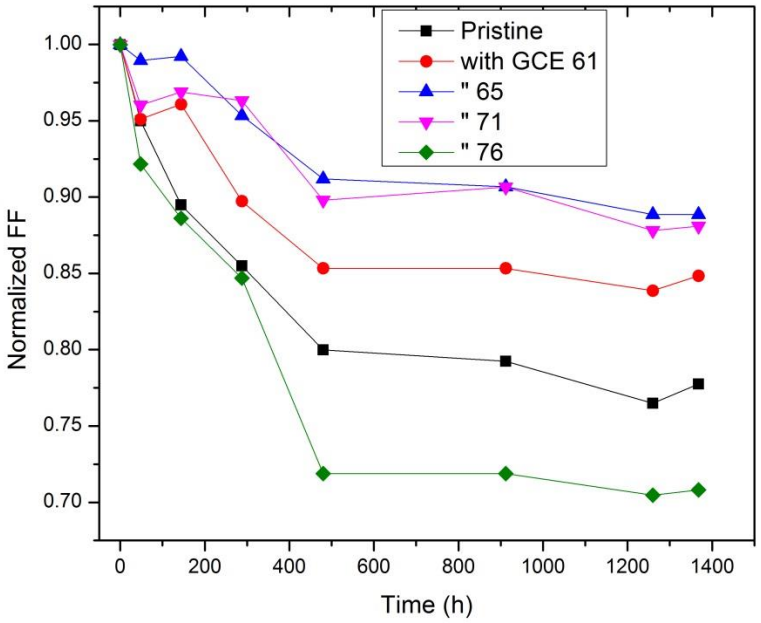

b)

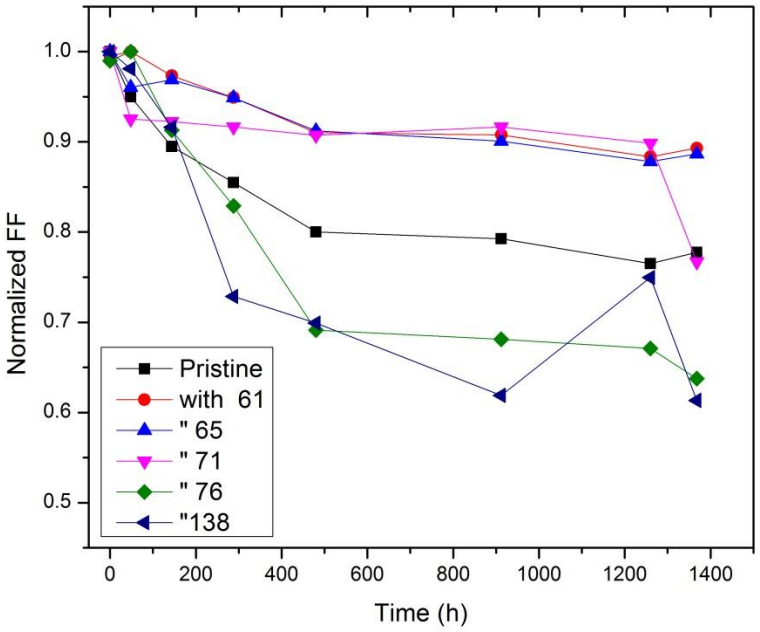

Figure 3.12. FF variation as a function of time for OPV devices ITO/PEDOT:PSS/P3HT:PCBM/FM encapsulated with Norland adhesives (61,62,71,76 and 138) inside a glove box a) covered with a glass plate and sealed and b) applying the adhesive directly on the cell. In both cases, adhesives were exposed to UV light.

a)

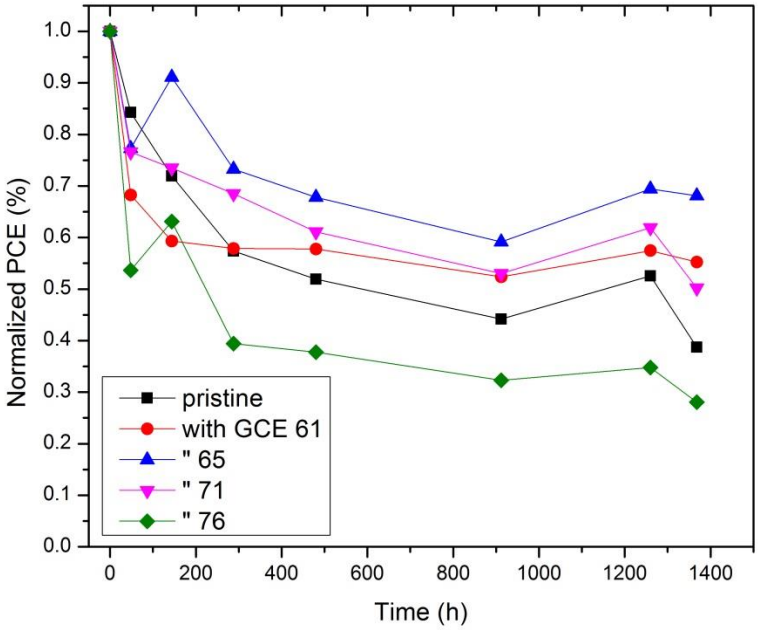

b)

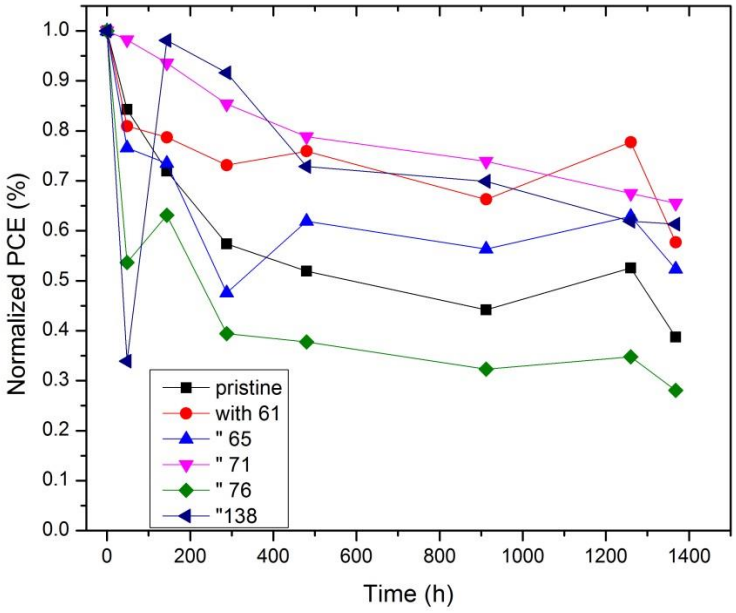

Figure 3.13. Normalized PCE variation as a function of time for OPV devices ITO/PEDOT:PSS/P3HT:PCBM/FM encapsulated with Norland adhesives (61,62,71,76 and 138) inside a glove box a) covered with a glass plate and sealed and b) applying the adhesive directly on the cell. In both cases, adhesives were exposed to UV light.

Table 3.2. Percentage of decay after 57 days of monitoring encapsulated OPVs devices (Under N_2 atmosphere) for the PV parameters: voltage, current density, FF and PCE, by using both, the direct and GCE procedures.

Procedures	Voltage	Current density	FF	PCE
GCE method	10%/NOA71	42%/NOA 71	30%/NOA 76	32%/NOA 65
Direct	2%/NOA 76	55%/NOA 76	11%/NOA 71	33%/NOA 71
Pristine	11%	42%	23%	62 %

In this case, the cells encapsulated with both methods degrade very similar because the presence of oxigen and water is kept very low inside of the glove box. As can be seen, OPVs encapsulated inside the glove box degrade less than those encapsulated outside the glove box; however, in both cases at the end of his lifetime, the encapsulated devices take longer time to degrade than pristine devices. Until day 40, OPVs encapsulated inside glove box degraded even more than OPVs encapsulated outside glove box (Figure 3.8), however, in the former case, OPVs kept in operation almost two times more that those encapsulated outside glove box.

OPVs were degraded in less degree with the adhesives NOA 65, with the GCE method, and NOA 71 when it was applied directly. Cells that decay less with each of the two methods are shown in Figure 3.14 when PCE for the encapsulated OPVs decreased 33% for direct encapsulation with NOA 71 and 32% with NOA 65 with the GCE method.

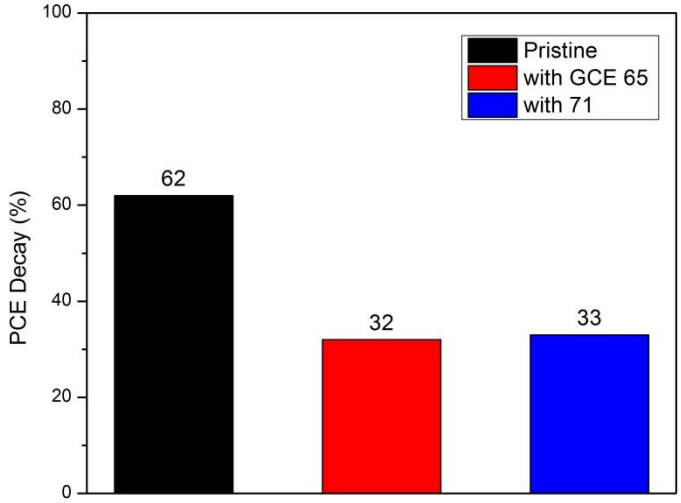

Figure 3.14. Efficiency of the OPVs encapsulated inside glovebox that degrade less after 80 days.

In Ref [31] the authors report one simple encapsulation method with a parafilm for organic optoelectronic devices with a structure ITO/PEDOT:PSS/P3HT:$PC_{71}BM$/LiF/Al, devices were based on ternary polymer solar cells. Parafilm (produced by the Pechiney Plastic Packaging Company) is a plastic film with a paper backing. Parafilm becomes soft and sticky at about 70 ℃, therefore the encapsulation process could be finished during the annealing treatment on PSCs. The power conversion efficiencies (PCE) of PSCs with and without encapsulation decrease 26% and 60% respectively, after 168 hours (7 days) of degradation under an ambient environment. This encapsulation method could be a competitive choice for organic optoelectronic devices, owing to its low cost and compatibility with flexible devices. In this thesis the PCE of encapsulated OPVs decrease 26 % after 300 h with GCE method using NOA 65 and 912 h with NOA 71 directly. OPVs without encapsulation showed a decrease of 60% after 1368 h. In Ref.

[39] authors use the adhesive Norland UV Sealant 91 for encapsulated devices with the ITO/PEDOT:PSS/PTB7:$PC_{71}BM$/TiOx/Al structure. Devices were covered with the UV sealant (except the electrodes) and then placing the glass slide on the top of the UV sealant. Encapsulation took place inside a glove box (under N_2 atmosphere) and stored outside. They were cured through UV light (20 W/m^2) for 30s. For the air stability test; after 20 days, the encapsulated PTB7:$PC_{71}BM$/TiOx based devices with optical sealant in a glove box and in air had an efficiency decay of about 32 %, and 42 %, respectively. For devices without sealant glass stored in air, the efficiency decay was approximately up 98 %. In this current thesis, the best Norland adhesives, whit the best lifetime, were by using NOA 65 and NOA 71 for GCE method and directly, respectively. The PCE for the encapsulated OPVs inside glovebox after 480 h with NOA 65 and 1200 h with NOA 71, decrease 32% in both cases. PCE for the encapsulated OPVs devices outside glovebox decreased 42% after 780 h with NOA 65 and 18% after 480 h with NOA 71.

Conclusions

In this thesis 5 different NOA adhesives (61,65,71,76 and 123) were compared when applied them to seal OPVs cells: two different encapsulating ways in two different atmospheres were used. For the best devices encapsulated under normal conditions, efficiency decays about 50% with NOA 65 and GCE method and 27% with NOA 71, in the direct form, while the pristine cell decays 64 %; all these facts after 46 days. On the other hand, for the best devices encapsulated inside a glove box (N_2 atmosphere), their efficiency decay about 32% using NOA 65 and 33% with NOA 71 using GCE procedure and directly, respectively. While the pristine cell decays 62%, all these test over 57 days. In both cases the adhesives that provided the best barrier protection for the devices were NOA 65 for cells encapsulated with the GCE technique and NOA 71 for devices encapsulated applying it directly onto the cathode side of the device.

These used adhesives for the OPVs encapsulation could be an effective option that would be worth further study. These adhesives could provide a good barrier protection for devices against degradation caused by water and/or oxygen upon exposure to air. Therefore the encapsulation methods with these adhesives are a competitive choice for OPVs cells, owing to their low cost, easy to use, compatibility with flexible devices and transparency. For future work is expected to perform the calculation of Water Vapor Transmission Rate (WVTR) and Oxygen Transmission rate (OTR) of these adhesives; also to use these adhesives under different OPVs configurations and sealing ways such as spin coating and doctor blading to create thin solid cover films.

References

[1] Jakaria Ahmad, et al. *"Materials and Methods for Encapsulation of OPV: A Review",* Renew Sustain Energy Rev 27: 104-17, 2013.

[2] Würfel Peter, "*Physics of Solar Cells : From Principles to New Concepts*." Physics of Solar Cells: 186, 2005.

[3] *Best research efficiencies chart*. 2016; Available from: http://www.nrel.gov/ncpv/

[4] Albert Polman, et al. *"Photovoltaic materials: Present efficiencies and future challenges"*, Science 352: 6283, 2016.

[5] Sean E. et al. *"Organic-Based Photovoltaics: Toward Low-Cost Power Generation",* MRS Bulletin 30: 10-15, 2005.

[6] Heliatek press release, Heliatek consolidates its technology leadership by establishing a new world record for organic solar technology with a cell efficiency of 13.02%, 2016, Available online: http://www.heliatek.com/en/press/press-releases/details/heliatek-sets-new-organic-photovoltaic-world-record-efficiency-of-13-2

[7] Huanqui Cao, et al. *"Recent Progress in Degradation and Stabilization of Organic Solar Cells",* J. Power Sources 264: 168-83, 2014.

[8] www.norlandprod.com/UVdefault.html

[9] International Energy Agency, *"CO2 Emissions from fuel combustion highlights"*, 2015.

[10] Antonio Luque and Steven Hegedus, *"Handbook of Photovoltaic Science and Engineering"*, Wiley, Great Britain, 2003.

[11] Wolfgang Tress, *"Device Physics of Organic Solar Cells"*, 1-384, 2011.

[12] C. W. Tang, et al. *"Two-ayer organic photovoltaic cell,"* Appl. Phys. Lett. 48, 2: 183–5, 1986.

[13] Travis L. Benanti, et al. "*Organic Solar Cells: An overview focusing on active layer morphology"*, Photosynth Res. 87: 73–81, 2006.

[14] Hyun Suk Jung, et al*. "Perovskite Solar Cells: From Materials to Devices",* Materials Views 11: 10-25, 2015.

[15] Frederik C. et al. "*25th Anniversary Article: Rise to Power – OPV-Based Solar Parks"*, Adv. Mater. 26: 29–39, 2014.

[16] J. C. Jean-Luc, et al. *"Molecular understanding of organic solar cells: The challenges,"* Acc. Chem. Res. , 42: 1691–99, 2009

[17] B. Kippelen, et al. *"Organic photovoltaics,"* Energy Environ. Sci, 2: 251–61, 2009.

[18] Hongkyu Kang, et al. *"Bulk-Heterojunction Organic Solar Cells: Five Core Technologies for Their commercialization"*, Adv. Mater, 2016.

[19] Jakaria Ahmad, et al. *"Materials and Methods for Encapsulation of OPV: A Review",* Renew Sustain Energy Rev 27: 104-17, 2013.

[20] S. Cros, et al. "*Definition of encapsulation barrier requirements: A method applied to organic solar cells",* Sol. Energy Mater. Sol. Cells 95: S65–9, 2011.

[21] Luca La Notte, et al. *"Influence of encapsulation materials on the optical properties and conversion efficiency of heat-sealed flexible polymer solar cells"*, Surface Coatings Tec 255: 69-73, 2014.

[22] Dan Yang, et al. *"Passivation Properties of UV-Curable Polymer for Organic Light Emitting Diodes",* ECS Solid State Letters 2 (9): 31-33, 2013.

[23] Kim N, et al. *"A correlation study between barrier film performance and shelf lifetime of encapsulated organic solar cells,"* Sol. Energy Mater. Sol. Cells 101: 140–6, 2012.

[24] R. Paetzold, et al. *"Permeation rate measurements by electrical analysis of calcium corrosion*", Rev. Sci. Instrum 74: 5147-50, 2007.

[25] Jens A. Hauch, et al. *"The impact of water vapor transmission rate on the lifetime of flexible polymer solar cells*", Appl. Phys. Lett. 93: 103306, 2008.

[26] Hee-Jae Lee, et al. *"Solution processed encapsulation for organic photovoltaics"*, Sol. Energy Mater. Sol. Cells 111: 97-101, 2013.

[27] Y. Kim, et al. *"Durable polyisobutylene edge sealants for organic electronics and electrochemical devices"*, Sol. Energy Mater. Sol. Cells 100: 120-5, 2012.

[28] D.M. Tanenbaum, et al. *"Edge sealing for low cost stability enhancement of roll-to-roll processed flexible polymer solar cell modules",* Sol. Energy Mater. Sol. Cells 97: 157-63, 2012.

[29] D. Elkington, et al. "*Single-Step Annealing and Encapsulation for Organic Photovoltaics Using an Exothermically-Setting Encapsulant Materia,.*" Sol. Energy Mater. Sol. Cells 124: 75-78, 2014.

[30] Hee-Jae Lee, et al. *"Solution processed encapsulation for organic photovoltaics",* Sol. Energy Mater. Sol. Cells 111: 97-101, 2013.

[31] Qian-Qian Sun, et al. "*A Simple Encapsulation Method for Organic Optoelectronic Devices."* Chin. Phys. B. 23(8): 083302, 2014.

[32] G. Dennler , et al. *"A new encapsulation solution for flexible organic solar cells"*, Thin Solid Films 511–2: 349-353, 2006.

[33] Smita Sarkar , et al. *"Encapsulation of organic solar cells with ultrathin barrier layers deposited by ozone-based atomic layer deposition",* Orga. Elect. 11: 1896–1900, 2010.

[34] Gayathri N. Kopanati, et al. *"Water Vapor Barrier Material by Covalent Self-Assembly for Organic Device Encapsulation",* Ind. Eng. Chem. Res. 53: 17894−900, 2014.

[35] Hasitha C. Weerasinghe , et al. *"Influence of moisture out-gassing from encapsulant materials on the lifetime of organic solar cells",* Sol. Energy Mater. Sol. Cells 132: 485–91, 2015.

[36] Martin Hermenau, et al. *"The effect of barrier performance on the lifetime of small-molecule organic solar cells"*, Sol. Energy Mater. Sol. Cells 97: 102–8, 2012.

[37] Jens Adams, et al. "*Air-processed organic tandem solar cells on glass: toward competitive operating lifetimes",* Energy Environ. Sci, 8: 169–76, 2015.

[38] Dan Yang, et al. *"Passivation Properties of UV-Curable Polymer for Organic Light Emitting Diodes*", ECS Solid State Letters 2 (9): 31-3, 2013.

[39] Tarek M. Abdel-Fattah, et al. *"Stability study of low and high band gap polymer and air stability of PTB7:PC71BM bulk heterojunction organic photovoltaic cells with encapsulation technique*", Synth. Met. 209: 348-54, 2015.

[40] Thien-Phap Nguyen, et al. *"Degradation of phenyl C61 butyric acid methyl ester: poly (3-hexylthiophene) organic photovoltaic cells and structure changes as determined by defect investigations",* JPE 2: 021013-1, 2012.

[41] Serap Gunes, "*Nanostructured Electrodes From Inorganic Materials for Hybrid Solar Cells, PhD thesis, Johannes Kepler Universit¨* at Linz, 2006.

[42] Matthew O. Reese, et al. "*Short-term Metal/Organic Interface Stability Investigations of Organic Photovoltaic Devices",* Sol. Energy Mater. Sol. Cells 92: 746, 2008.

[43] B. Ray, et al. *"A compact physical model for morphology induced intrinsic degradation of organic bulk heterojunction solar cell,"* Appl. Phys. Lett.. 99(3): 033303, 2011.

[44] Q.L. Song, et al. "*Degradation of small-molecule organic solar cells",* Appl. Phys. Lett. 89: 251113, 2006.

[45] Nadia Grossiord, et al. *"Degradation mechanisms in organic photovoltaic devices"*, Orga. Elect. 13: 432-56, 2012.

[46] Wallace C. H. Choy*, "Organic solar cells; Material and device physics",* 2013.

[47] Christoph Brabec, et al. "*Organic Photovoltaics: Materials, Device Physics, and Manufacturing Technologies*", 2009.

[48] Enrique Pérez-Gutiérrez, et al. *"Titanium Oxide : Fullerene Composite Films as Electron Collector Layer in Organic Solar Cells and the Use of an EasyDeposition Cathode***."** Opt. Mater. 36: 1336–41, 2014.

[49] Matthieu Manceau, et al. *"Effects of long-term UV–visible light irradiation in the absence of oxygen on P3HT and P3HT:PCBM blend",* Sol. Energy Mater. Sol. Cells 94: 1572-77, 2010.

[50] Armando Álvarez-Fernández, et al. "*Performance and stability of PTB7:PC71BM based polymer solar cells, with ECZ and/or PVK dopants, under the application of an external electric field"*, J Mater Sci: Mater Electron, 27: 6271–81, 2016.

[51] Kwang-Ryul Kim, et al*. "Rapid laser fabrication of microlens array using colorless liquid photopolymer for AMOLED devices",* Opt. Commun 284: 405–410, 2011.

[52] Zhao Xu-Liang, et al. *"Optimized design and fabrication of nanosecond response electro optic switch based on ultraviolet-curable polymers*", Chin. Phys. B, 4: 044101, 2015.

[53] Kuo-Yung Hung, et al. "*Optimum electrostatic force control for fabricating a hybrid UV-curable aspheric lens",* J. Micromech. Microeng, 20: 075001, 2010.

[54] I.-J. No, el at. *"Fabrication and characteristics of organic thin-film solar cells with active layer of interpenetrated hetero-junction structure"*, J. Appl. Phys. 4: 83–90, 2012.

[55] P. Boland, et al. *"Investigation of structural, optical, and electrical properties of regioregular poly(3-hexylthiophene)/fullerene blend nanocomposites for organic solar cells"*, Thin Solid Films 518: 1728–31, 2010.